International Journal of Modern Physics B, Vol. 11, No. 12 (1997) 1411–1444

THE BAK–SNEPPEN MODEL: A SELF-ORGANIZED CRITICAL MODEL OF BIOLOGICAL EVOLUTION

NING-NING PANG
Department of Physics, National Taiwan University, Taipei, Taiwan, R.O. China

Received 15 October 1996

Recently, Bak and Sneppen proposed a simple model, the Bak–Sneppen (BS) model, as a coarse-grained description of biological evolution. It has attracted a lot of attention from interdisciplinary statistical physics community, for its simple model definition but extremely rich properties to be explored. The aim of this paper is to give a pedagogical and update review of this fast-developing topic. The emphasis is on the mechanism by which the BS model approaches the self-organized critical state, the universal properties of the system at criticality, and the relation with other topics, such as directed percolation, random walk, and a few self-organized critical models.

1. Introduction

Since Bak and Sneppen[11] proposed a self-organized critical (SOC) model, known as the "Bak–Sneppen Model", to account for the characteristic intermittency of actual evolution and the scale invariance of extinction events,[50] it has attracted much attention from the statistical community,[22] not only because of the simplicity in the model definition but also the rich statistical behaviors in which it contains.[43] Although this model is definitely oversimplified for describing the real biological evolution, it has the merit of developing complexity out of simplicity, as pointed out in Ref. 55. Looking back at the history about the applications of directed percolation, Grassberger[18] has commented that the Bak–Sneppen model, sufficiently simple to be paradigmatic, will sooner or later find its wide applications.

The aim of this paper is to give a pedagogical and current review of this fast-developing topic. Instead of digging out the details form the biological aspect (see, for example, Refs. 4 and 50), I shall concentrate on the mechanism by which the BS model approaches the self-organized critical state, the universal properties of the system at criticality, and the relation with other topics. This article is organized as follows. In Sec. 1, I begin with a brief review on the link between the Bak–Sneppen evolution model and the fossil record. I then explore, in Sec. 2, the mechanism by which the Bak–Sneppen evolution model approaches the self-organized critical state.

PACS Nos: 05.40.+j, 87.10.+e

Then, in Sec. 3, the focus is on the universal properties of the system at criticality, in particular, the geometric properties of avalanches, the spatial-temporal correlations between successive events, and fractal pattern in the space-time plot. In Sec. 4, the random neighbor variant of the BS model is reviewed. The exact treatment of the random neighbor variant gives a very good example for pedagogical purpose. Section 5 discusses the relation of the BS model to other topics, such as

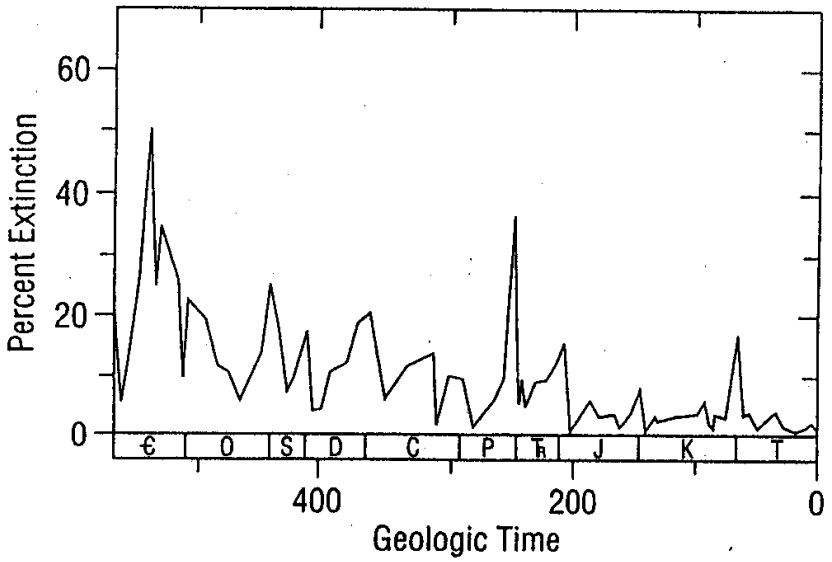

(a)

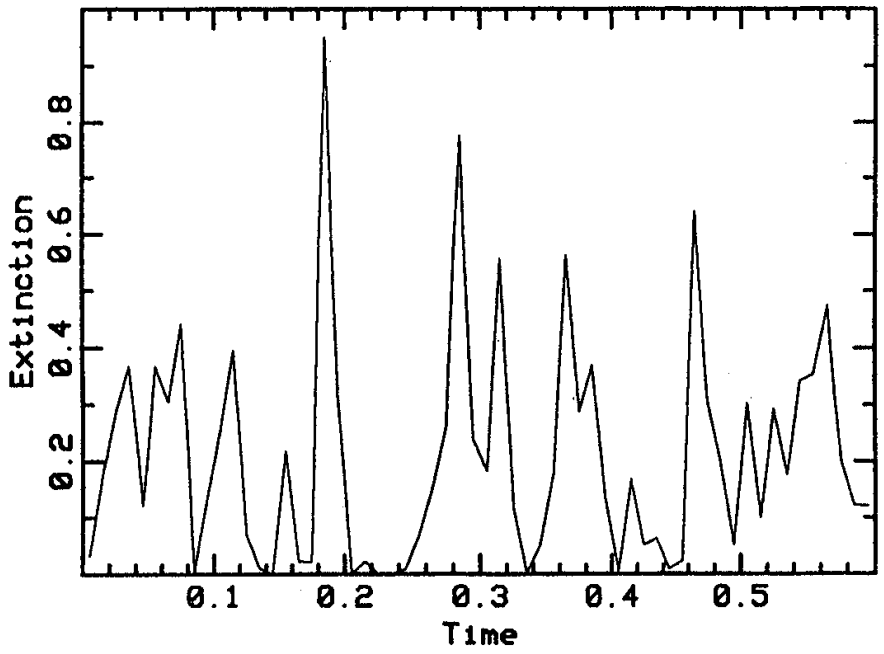

(b)

Fig. 1.1. (a) Temporal evolution of extinctions recorded over the last 600 million years, as given by J. Sepkoski.[49] The ordinate shows estimates of the percentage of species that went extinct within intervals of 5 million years. (b) Temporal evolution of the "mutation" activity of species for the model with 200 "species" and a mutation rate parameter $T = 0.01$, as given by Sneppen *et al.*[50]

directed percolation, random walk, and a few self-organized critical models, and the subtle differences between them. Section 6 concludes with comments and discussions of some open questions and possible directions for future investigation.

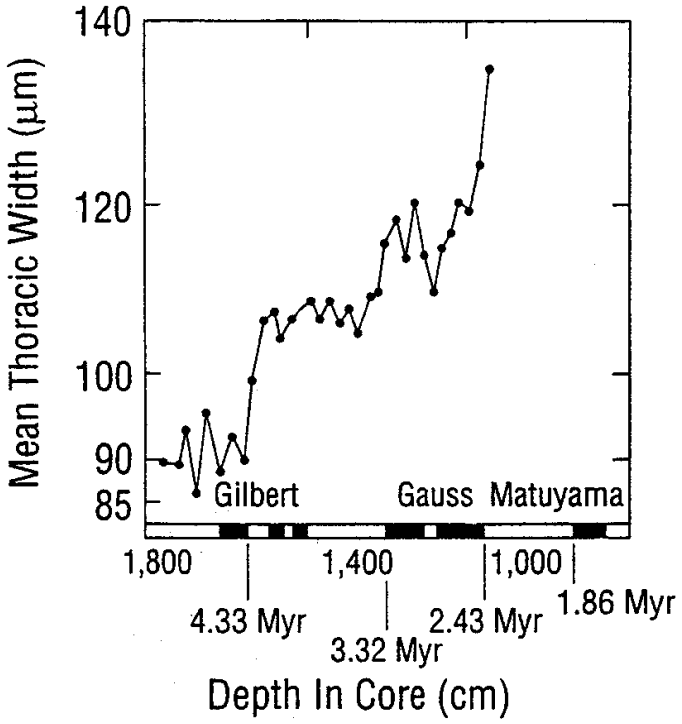

(a)

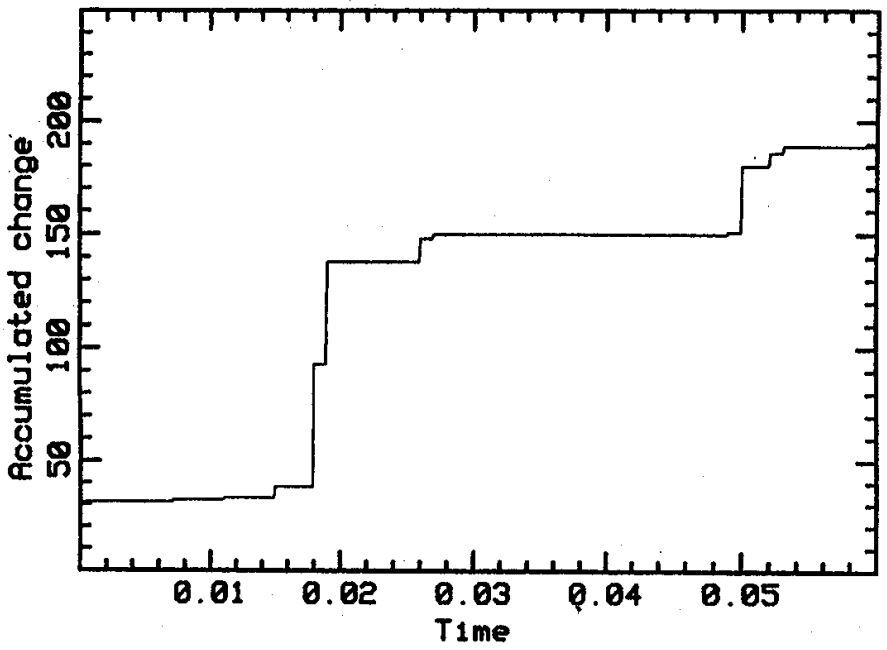

(b)

Fig. 1.2. (a) Time series for the variation of the morphology of a single species. The figure shows the increase in thoracic width of the Antarctic radiolarian *Pseudocubus vema* during 2.5 million years, as given by Kellog.[26] (b) Model prediction of time series for change of single species morphology, estimated as its accumulated mutation activity, as given by Sneppen *et al.*[50]

1.1. *The biological motivation*

Since the theory of gradualism, which expects biological evolution takes place in a smooth and gradual manner, was proposed in the early twentieth century, this concept has dominated the realm of paleontology.[4] Not until recent years, by studying the stratigraphic records of 19897 fossil genera, Raup, Sepkoski, and Boyanian[44,45,48,49] revolutionarily gave strong evidence that biological evolution takes place in terms of intermittent bursts of activity with long periods of stasis. The

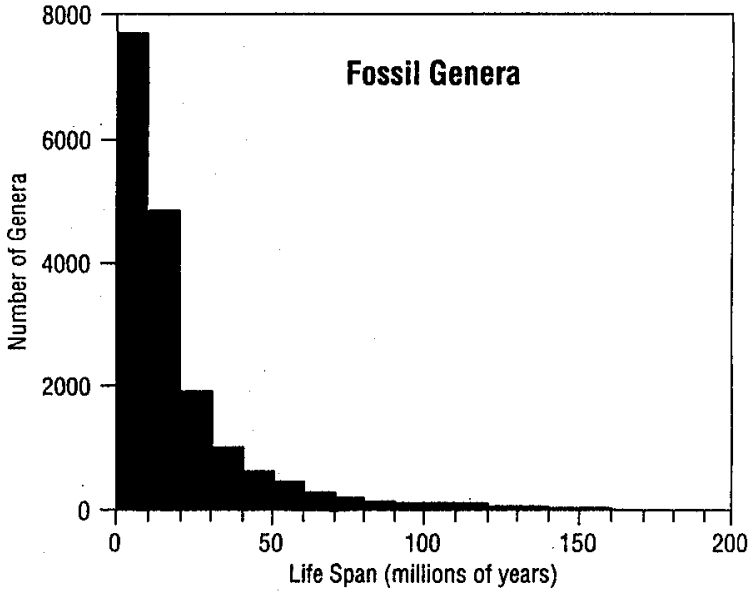

(a)

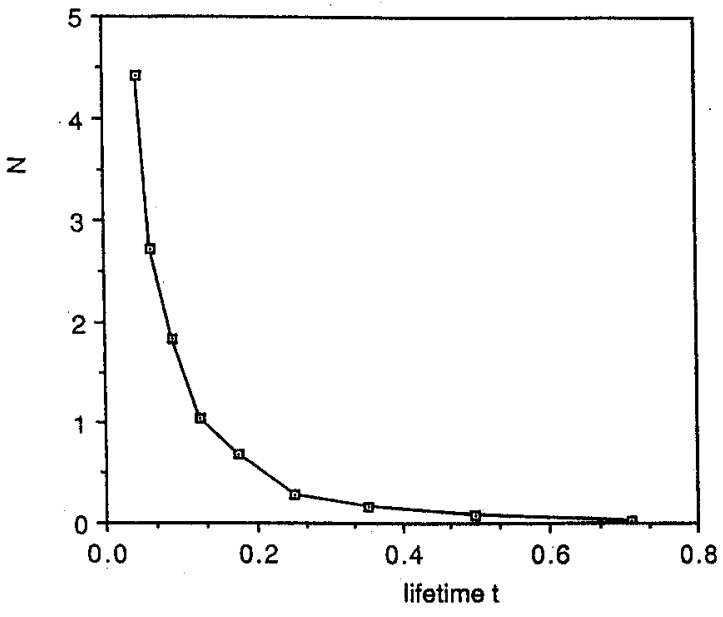

(b)

Fig. 1.3. (a) Lifetime distribution for species, as recorded by Raup.[44] The distribution can be well fit by a power law $N(t) \sim 1/t^2$. (b) Distribution of lifetime for the model with a mutation rate parameter $T = 0.001$, as given by Sneppen *et al.*[50]

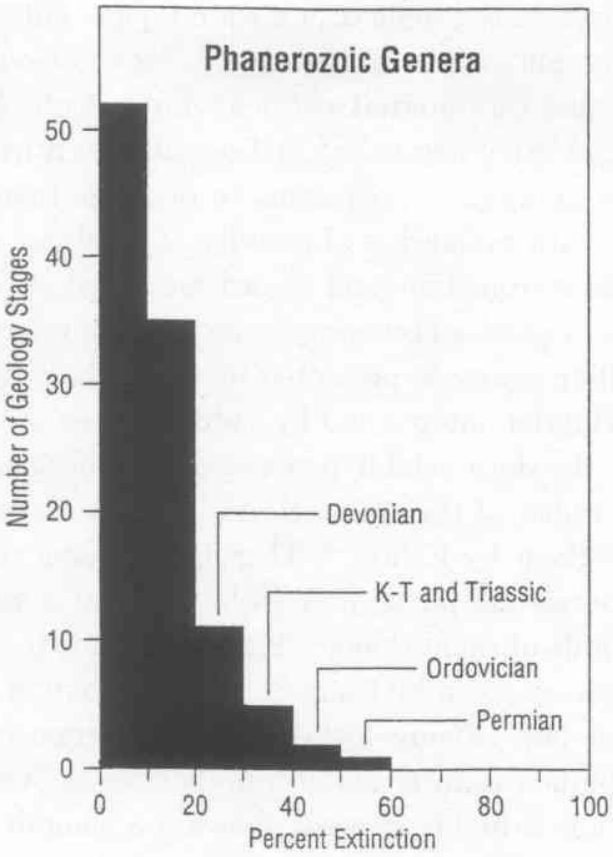

(a)

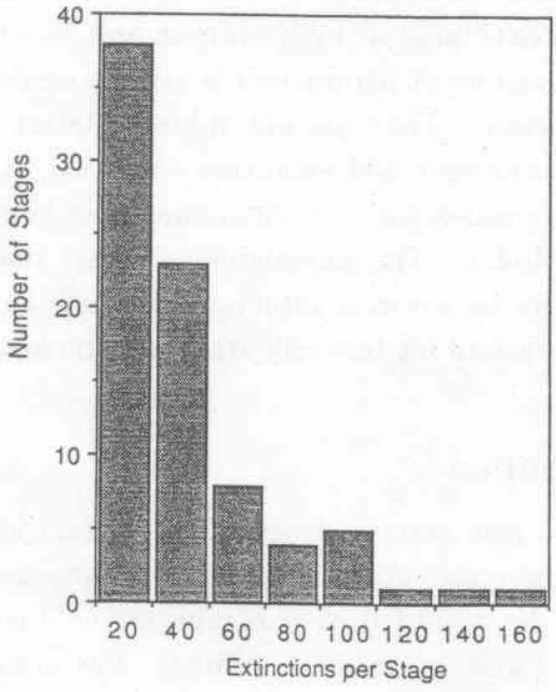

(b)

Fig. 1.4. (a) Histogram of extinction events from Fig. 1.1(a), as shown by Raup.[44] The data are binned in intervals of 5 million years over the last 600 million years. (b) Histogram of mutation activity predicted by the random neighbor variant (see Sec. 4 for definition) of the BS model, as given by Sneppen *et al.*[50]

magnitudes of the bursts may extend over a wide range. This intermittent behavior has been coined in the phrase *punctuated equilibrium* by Gould and Eldredge.[19] It has been conjectured that this intermittent behavior indicates biological evolution to a self-organized critical (SOC) state.[6,27] Self-organized critical behaviors[12,13] refer to the tendency of large dynamical systems to organize themselves into a critical nonequilibrium state with avalanches of activity of all sizes.

Some pertinent data from the fossil record are listed as follows. Figure 1.1(a) shows the percentage of species becoming extinct within intervals of 5 million years over the last 600 million years, as presented by Sepkoski.[49] There are long periods of relatively little extinction interrupted by sudden bursts of large peaks representing mass extinction: the data exhibit *punctuated equilibrium.* Figure 1.2(a) is the increase in thoracic width of the Antarctic radiolarian *Pseudocubus vema* during 2.5 million years, as given by Kellog.[26] This figure shows the time series for the variation of single species morphology. We observe that a series of three plateaus are separated by periods of rapid change. Figure 1.3(a) is the histogram of lifetime distribution for species, as given by Raup.[44] The distribution of life-span can be fit quite well by a power law. Figure 1.4(a) is the histogram of extinction distribution. The data are binned in intervals of 5 million years over the last 600 million years. The distribution is highly skewed, showing a smooth variation from many periods having little extinction to a few periods with large extinction percentages. Figures 1.3(a) and 1.4(a) indicate the self-organized critical behavior.

There have been several attempts to explain the above observation theoretically by constructing mathematical models, e.g., the model "Game of Life" by Bak, Chen, and Creutz,[6] and the "NKC models" by Kauffman and Johnsen.[27] However, in these models, some external tuning of parameters is always needed in order to bring the system to the critical state. They are not robust against small changes, as they should be in order to represent real evolution. In 1993, Bak and Sneppen[11] presented for the first time a self-organized critical model of biological evolution, known as the "Bak–Sneppen Model". This model demonstrates that large catastrophic extinctions, not necessarily by external intervention (such as meteorites), can occur as the natural consequence of intrinsically statistical biological mechanisms.

1.2. *The model definition*

The BS model[11] is a coarse-grained description of biological evolution, i.e. a description on a large time scale. An entire species is represented by a single fitness parameter, which can be regarded as a complex combination of factors such as genetic materials and forces of natural habitat. The stability of each species is characterized by a barrier height. The barriers are the measure of stability. A jump across a barrier can be thought of as either a mutation of a species or the substitution of one species by a better one in an ecological niche. Since the smallest barriers are related to the lowest fitness and the highest barriers correspond to the highest fitness, the barriers are also a measure of fitness. In addition, the fitness

of each species is affected by other species to which it is coupled in the ecosystem. Therefore, when a species makes an adaptive move, it changes the fitness landscapes of its neighbors.

In order to capture the above salient features, the model is specified by the following dynamical rules[11]: (1) N species are arranged on a one-dimensional line with periodic boundary conditions; (2) a random barrier B_i, equally distributed between 0 and 1, is assigned to each species; (3) at each time step, the ecology is updated by locating the site with the lowest barrier $B_{\min}$, mutating it by assigning a new random number to that site, and changing the landscapes of the two nearest neighbors by assigning new random numbers to those sites too.

Due to the principal characteristic in the updating rule, i.e. the global search of the minimals, the system, started with arbitrary initial configurations, after the extensive transient period will reach the *critical stationary state.*[11] Although this model is definitely oversimplified as a description of true biological evolution, it does provide a possible explanation for the characteristic intermittency of actual evolution and the scale invariance of extinction events in the fossil record, studied by Raup *et al.*[44,45,48,49]

1.3. *Comparison with the fossil record*

The time unit in the BS model is identified with an evolutionary step. It does not correspond to real physical time. So far, there are two ways of introducing a real time scale into the BS model in the literature (Refs. 52 and 50). Schmoltzi and Schuster[52] construct at each time step a local stochastic updating rule by introducing a new random variable η_i, which models all not explicitly known degrees of freedom of the system. If the random barrier B_i is smaller that η_i, then the site i and its two nearest neighbors are updated. By Contrast, Sneppen *et al.*[50] conjectured the time scale for trasversing a barrier of the height B_i is exponentially proportional to the barrier height, i.e. $\Delta t_i \sim \exp(B_i/T)$, based on the rugged fitness landscape picture.[25,16,8] Here T represents an effective mutation rate parameter defining the time scale of mutations. Hence, the local probability of jumping over a barrier is $\exp(-B_i/T)$. By either one of these two methods, it is possible to observe time steps in which no evolution occurs and its duration does obey a power law distribution.

To demonstrate that the BS model does provide a possible explanation for the characteristic intermittency of actual evolution and the scale invariance of extinction events, the corresponding plots [Figs. 1.1(b), 1.2(b), 1.3(b) and 1.4(b)] from numerical simulation of the BS model[50] are exhibited in the following, compared to the data of fossil records [Figs. 1.1(a), 1.2(a), 1.3(a) and 1.4(a)], respectively. Figure 1.1(b) shows temporal evolution of the "mutation" activity of species for the model with 200 "species" and a mutation rate parameter $T = 0.01$. The figure shows the intermittency of evolutionary activities with a few large peaks representing mass extinction and many small peaks representing relatively milder extinction

events. Figure 1.2(b) is the time series from the change of a single species morphology, estimated as its accumulated number of mutations. It shows the behavior of punctuated equilibrium. Figure 1.3(b) is the measure of lifetime as the interval between successive mutational events of a given species. Figure 1.4(b) is the histogram of global distribution of the number of mutations of species occuring. Both Figs. 1.3(b) and 1.4(b) obey power law distributions. These plots [Figs. 1.1(b), 1.2(b), 1.3(b) and 1.4(b)] all have the behaviors qualitatively similar to the data from fossil records [Figs. 1.1(a), 1.2(a), 1.3(a) and 1.4(a)], respectively.

Since the BS model is a coarse-grained description of biological evolution, i.e. a description on a large time scale and one single fitness parameter representing a combination of all factors of genetic materials and influences of natural habitat, therefore, this model cannot be asked to reproduce any specific event that is actually observed in nature. It must be considered only on a statistical level. In the following sections, I will move on to the aspect of self-organized criticality inherent in the BS model.

2. The Mechanism of Self-Organized Processes

2.1. *Avalanches*

The evolution of self-organized criticality usually takes places through bursts of avalanches.[31] An avalanche[31] is defined by a sequence of evolution events started at any integer time $s = s_0$ where the minimum random barrier $B_{\min}(s = s_0)$ is denoted by p. This avalanche is terminated at the first time s' where the minimum random barrier $B_{\min}(s')$ is larger than p; i.e. for all times s with $s_0 < s < s'$, the evolution events have $B_{\min}(s) < p$. Assume that at a certain time, p is the minimal barrier and all other barriers are larger than p. An avalanche (defined by p) starts at this site, and new random numbers are given to this site and the nearest neighbors. If one or more of the new random numbers is less than p, then those sites which were activated by the initial minimal site must be the next activated. The avalanche terminates when all the sites activated with barriers less than p are eliminated. Then, at the next step, the minimal site must have a barrier larger than p.

We see that all activated sites are connected, and an avalanche is independent of the random environment at and before the time when the avalanche started. Note that at every time an avalanche is started, and big avalanches contain smaller ones. Therefore, there is a hierarchy of avalanches, defined by their respective thresholds. Figure 2.1 is the plot of $B_{\min}(s)$ versus time s with system size $N = 4096$ in a small time zone. It illustrates the hierarchical feature of avalanches, i.e., the structure of subavalanches within the avalanches.

An avalanche is characterized by two principal numbers s and n_{cov},[32] the avalanche size and the number of activated sites, respectively. By definition, the avalanche size equals its temporal duration. Because of the connected nature of the set of activated sites, n_{cov} equals the avalanche spatial extent b. When an avalanche

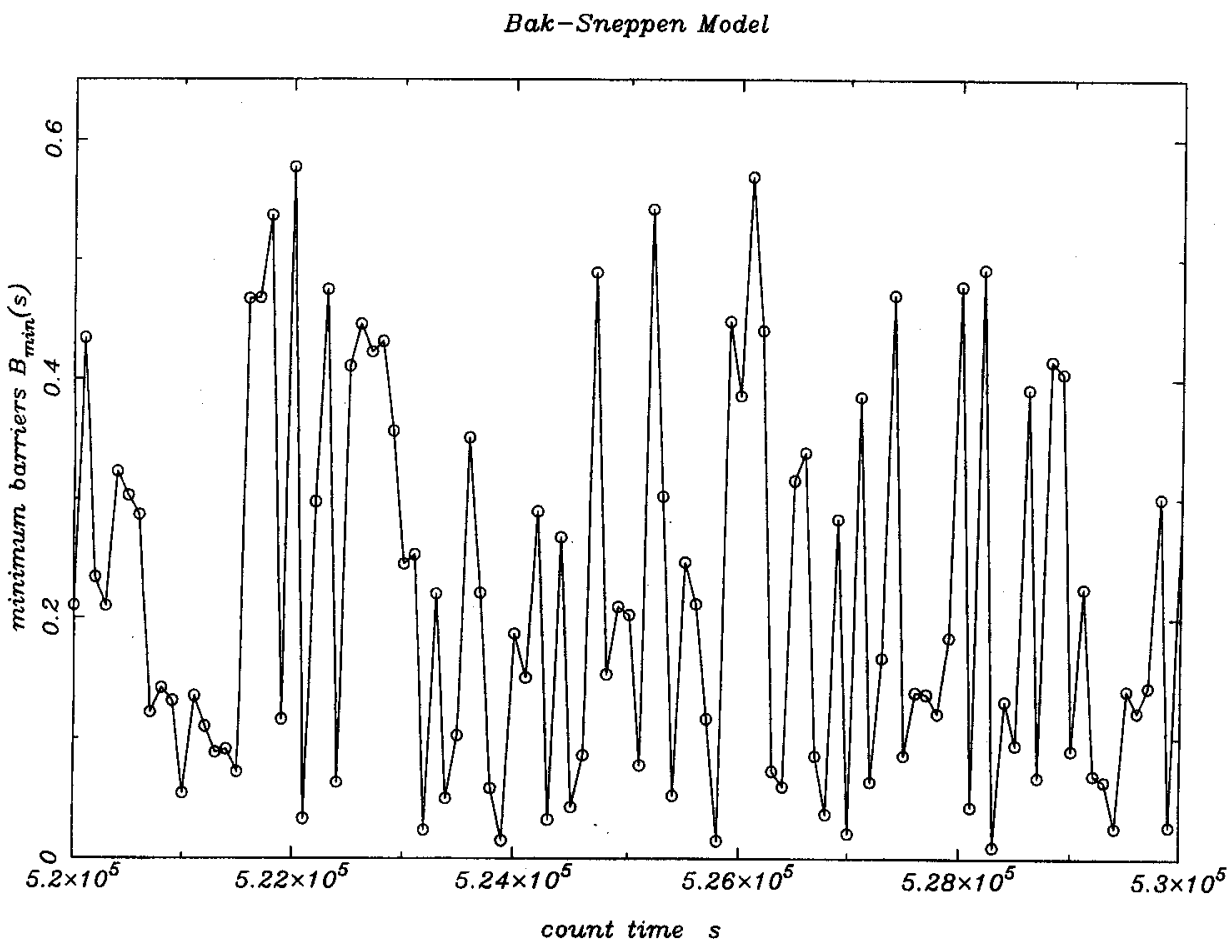

Fig. 2.1. The minimum barrier $B_{\min}(s)$ versus time s in the BS model with system size $N = 4096$ in a small time zone. Note the structure of subavalanches within the avalanches.

(defined by p) is terminated, the barriers B_i on the set of activated sites are uncorrelated and uniformly distributed between p and 1. In addition, it is important to note that the events within the same avalanche are spatially and temporally correlated but two subsequent avalanches are mutually uncorrelated. The spatial-temporal correlation between events will be further discussed in the next section.

2.2. *The "gap" function*

Paczuski *et al.*[42] have proposed a "gap" equation to describe how the system self-organizes itself into the critical state. The gap, $p_{\min}(s)$, is defined[42] as the largest of the minimal $B_{\min}$ which have been selected up to time s. It is an increasing function of time, with flat plateaus that become larger and larger. $p_{\min}(s)$ can not increase until all sites activated with $B_i < p_{\min}(s)$ are eliminated through subsequent selection and update. Figure 2.2 shows the gap $p_{\min}(s)$ as an envelope function that tracks the increasing peaks in $B_{\min}$.[43] On the average, the gap jumps by an amount $(1 - p_{\min})/N$, where N is the system size. The number of time steps separating events when the gap jumps to its next higher value, i.e. the width of a plateau, is the size of an avalanche, defined by $p_{\min}(s)$. Thus, the mechanism of

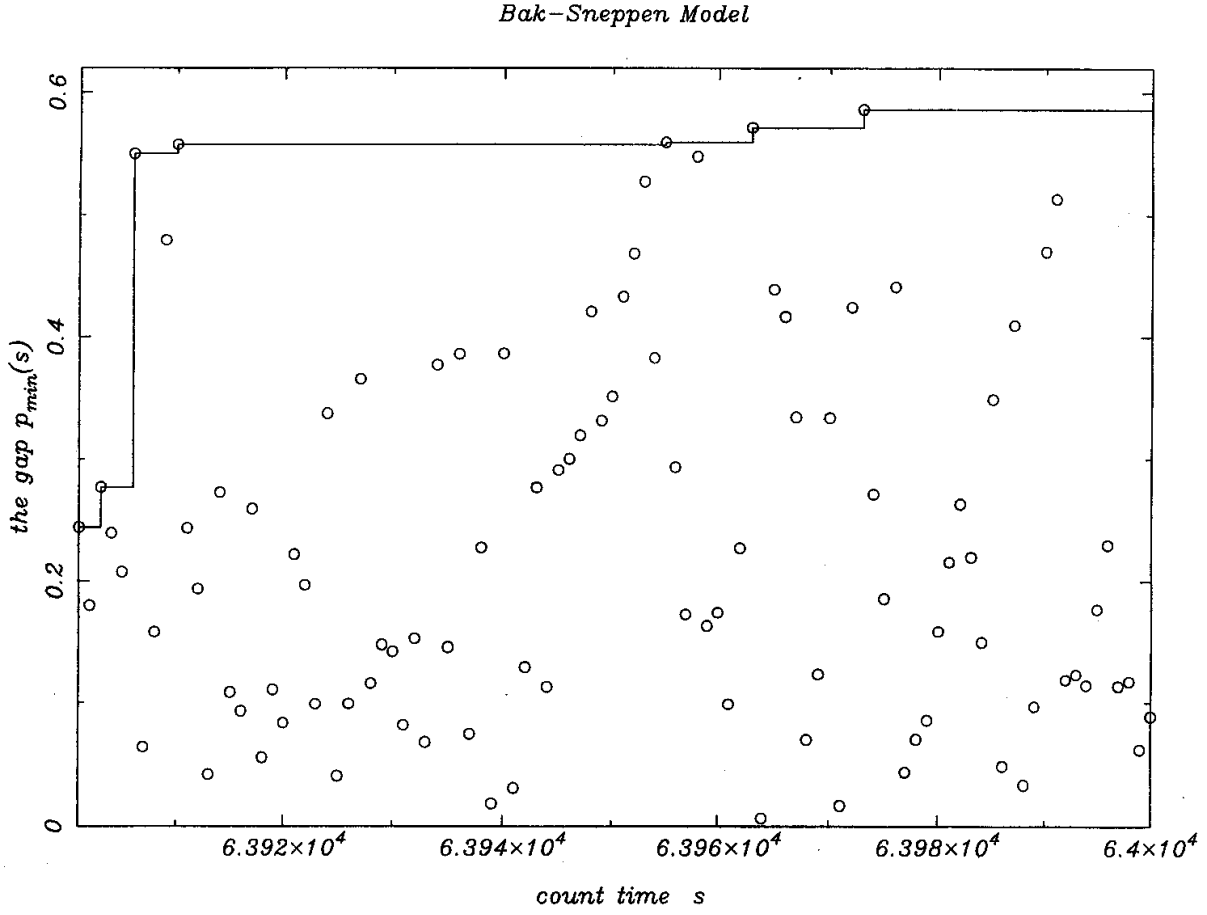

Fig. 2.2. This figure illustrates the gap $p_{\min}(s)$ being the largest of the minimal $B_{\min}$ which have been selected up to time s.

self-organization can be described by the "gap" equation[42]:

$$\frac{d\langle p_{\min}\rangle}{ds} = \frac{1-\langle p_{\min}\rangle}{N\langle s\rangle_{p_{\min}}}, \tag{2.1}$$

where the angular brackets denote the average over randomness and $\langle s\rangle_p$ is the average size of an avalanche defined by p.

Here, I will digress a little bit in order to show the importance of the interaction between neighbors in the updating rules for the BS model to reach the critical state. Let us define the noninteractive variant by the same updating rules of the BS model except that there is no coupling between the nearest neighbors. That is, when the minimal site is located, the updating is done by assigning a new random number to this site without changing the barriers of the two nearest neighbors. For the noninteractive variant, we can easily obtain

$$\langle s\rangle_{p_{\min}} = \frac{\sum_s s p_{\min}^s}{\sum_s p_{\min}^s} = \frac{p_{\min}}{1-p_{\min}}. \tag{2.2}$$

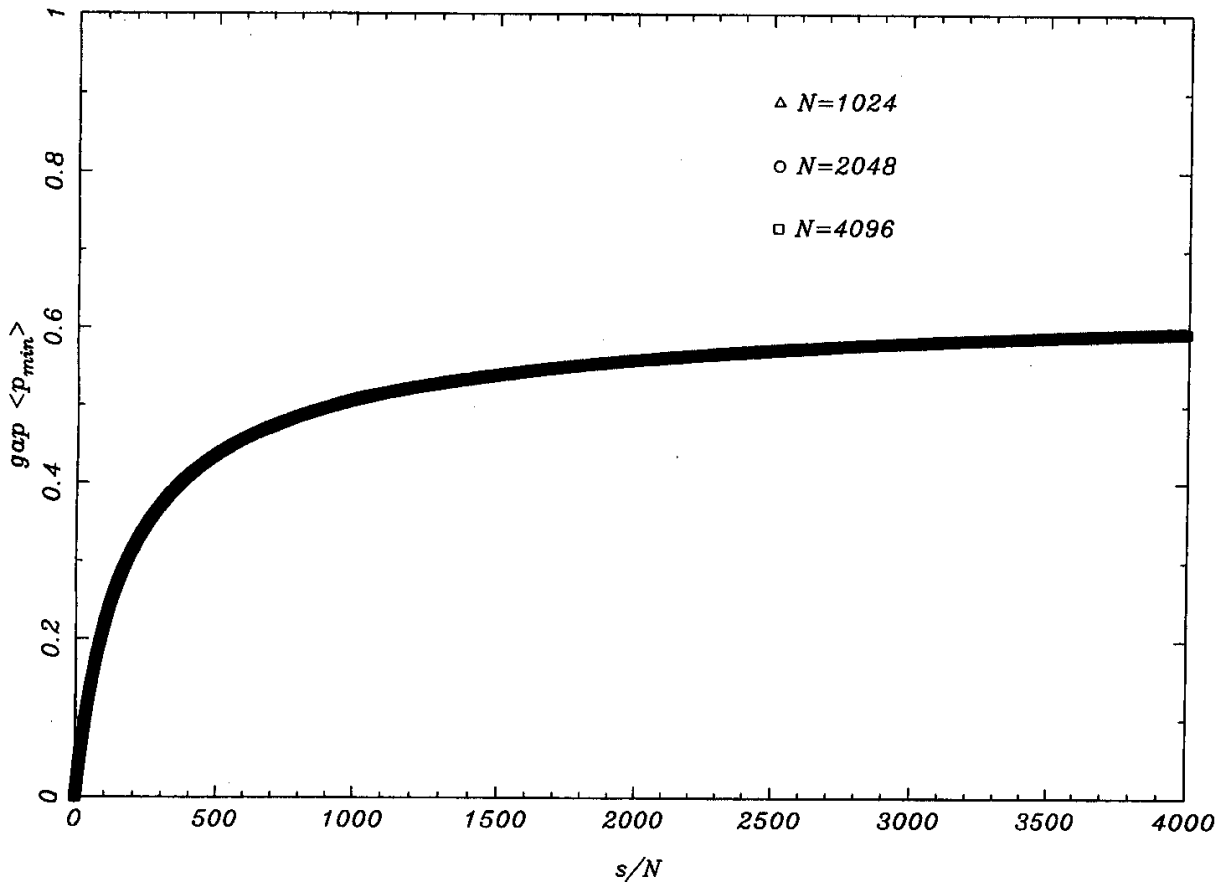

Fig. 2.3. The data collapse of the gap $p_{\min}$ versus s/N with system size $N = 1024$, 2048, and 4096 in the time durations $s = 16000$, 32000 and 64000, respectively, in the BS model.[40]

The average avalanche size $\langle s \rangle_{p_{\min}}$ of the noninteractive variant increases as the gap $p_{\min}$ increases. When $p_{\min} \to 1$, $\langle s \rangle_{p_{\min}}$ eventually diverges and, therefore, $dp_{\min}/ds = 0$. Henceforth, the noninteractive variant will reach a "dead" state with all barriers equal to 1.

For the Bak–Sneppen Model, in contrast, the inclusion of the nearest neighbor interaction in the updating rules enables the reduction of the high barriers and, therefore, suppresses the increase of the gap $p_{\min}(s)$. Numerical studies[42] show that the average avalanche size $\langle s \rangle_p$ diverges as $p \to p_c$, where $p_c = 0.667 \pm 0.001$. That is, after an extensive transient period, the system reaches the stationary state. All mutations turn out to take place through barriers which are less than p_c. Near p_c, the average avalanche size behaves as $\langle s \rangle_p \sim (p_c - p)^{-\gamma}$,[42] in the range of avalanche spatial extent $\langle b \rangle_p$ much less than system size N. Then, Eq. (2.1) can be integrated to give

$$\frac{s}{N} \sim \int (p_c - \langle p_{\min} \rangle)^{-\gamma} (1 - \langle p_{\min} \rangle)^{-1} d\langle p_{\min} \rangle .$$

Consequently,

$$(p_c - \langle p_{\min} \rangle) \sim \left(\frac{s}{N} \right)^{-\rho}, \quad \rho = \frac{1}{\gamma - 1}. \tag{2.3}$$

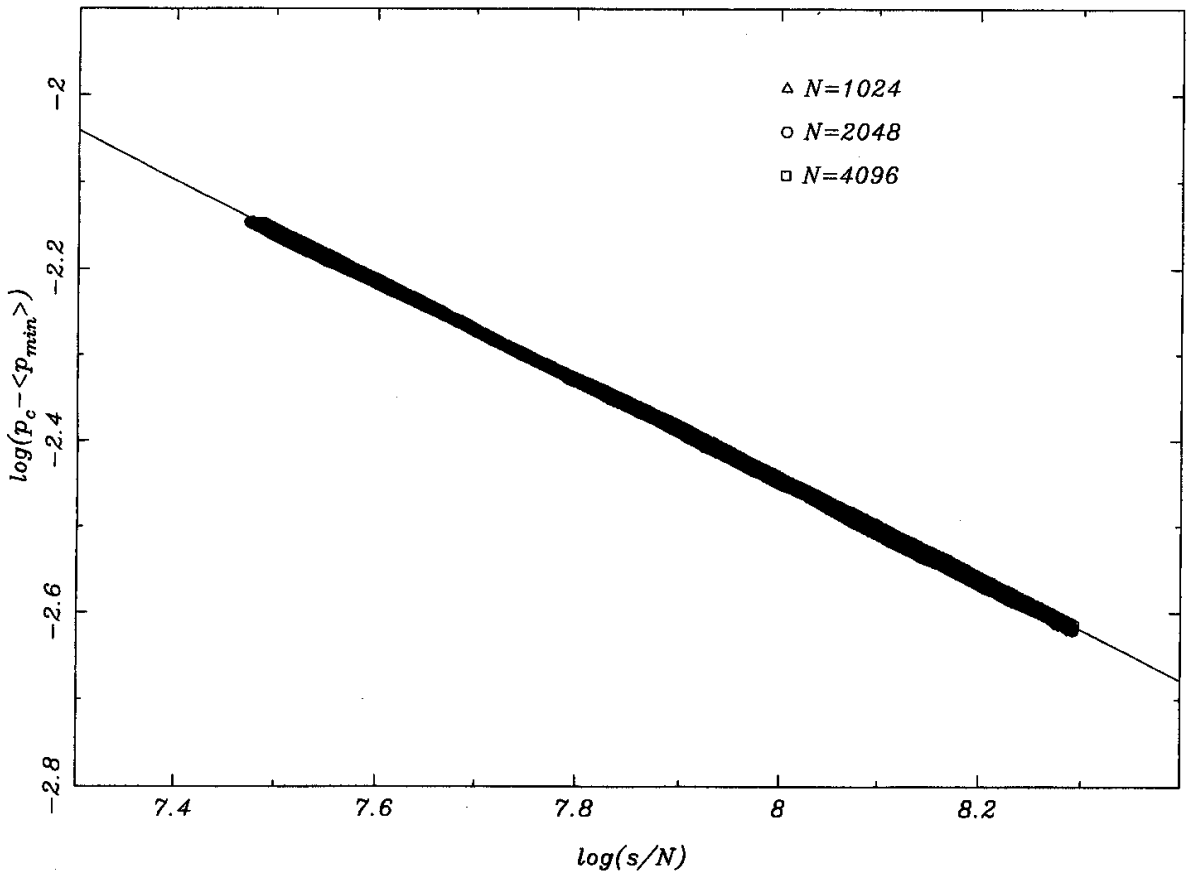

Fig. 2.4. The log–log plot of $(p_c - p_{\min})$ versus s/N with system sizes $N = 1024$, 2048, and 4096 in the time durations $s = 16000$, 32000, and 64000, respectively, in the BS model.[40] The straight line fit by least squares to the data gives $\rho = 0.56 \pm 0.02$, in agreement with the theoretical prediction $\rho = 0.59 \pm 0.03$ based on the exponent $\gamma = 2.7 \pm 0.1$ in Ref. 23.

The numerical studies[40] have confirmed the above prediction[42] about the scaling behaviors of the gap $p_{\min}(s)$ near the critical point p_c. Figure 2.3 gives excellent data collapse of the gap $p_{\min}$ versus s/N.[40] Figure 2.4 is the log–log plot of $(p_c - \langle p_{\min} \rangle)$ versus s/N.[40] The straight line fit by least squares to the data gives $\rho = 0.56 \pm 0.02$, in agreement with the theoretical prediction $\rho = 0.59 \pm 0.03$ based on the exponent $\gamma = 2.7 \pm 0.1$ in Ref. 23.

Next, consider the distributions of the barriers $P(B_i)$ and minimum barriers $P(B_{\min})$ as functions of barrier heights B_i and $B_{\min}$, respectively. The system starts from an initial state where the distribution of barriers $P(B_i)$ is uniformly distributed over $[0, 1)$. Since the minimal site is always updated at each time step, the sites with low barrier heights become rare. In addition, because new random barriers are always drawn from a uniform distribution, the distribution $P(B_i)$ should resemble a step function. Thus, as the gap $p_{\min}(s)$ increases with time s, the distribution $P(B_i)$ vanishes for $B_i < p_{\min}(s)$ and is a constant over the range $[p_{\min}(s), 1)$. After an extensive transient period, the system reaches the critical state and the distribution $P(B_i)$ becomes stationary, uniformly distributed between p_c and 1. The distribution of minimum barriers $P(B_{\min})$ in the critical state can be obtained by the concept

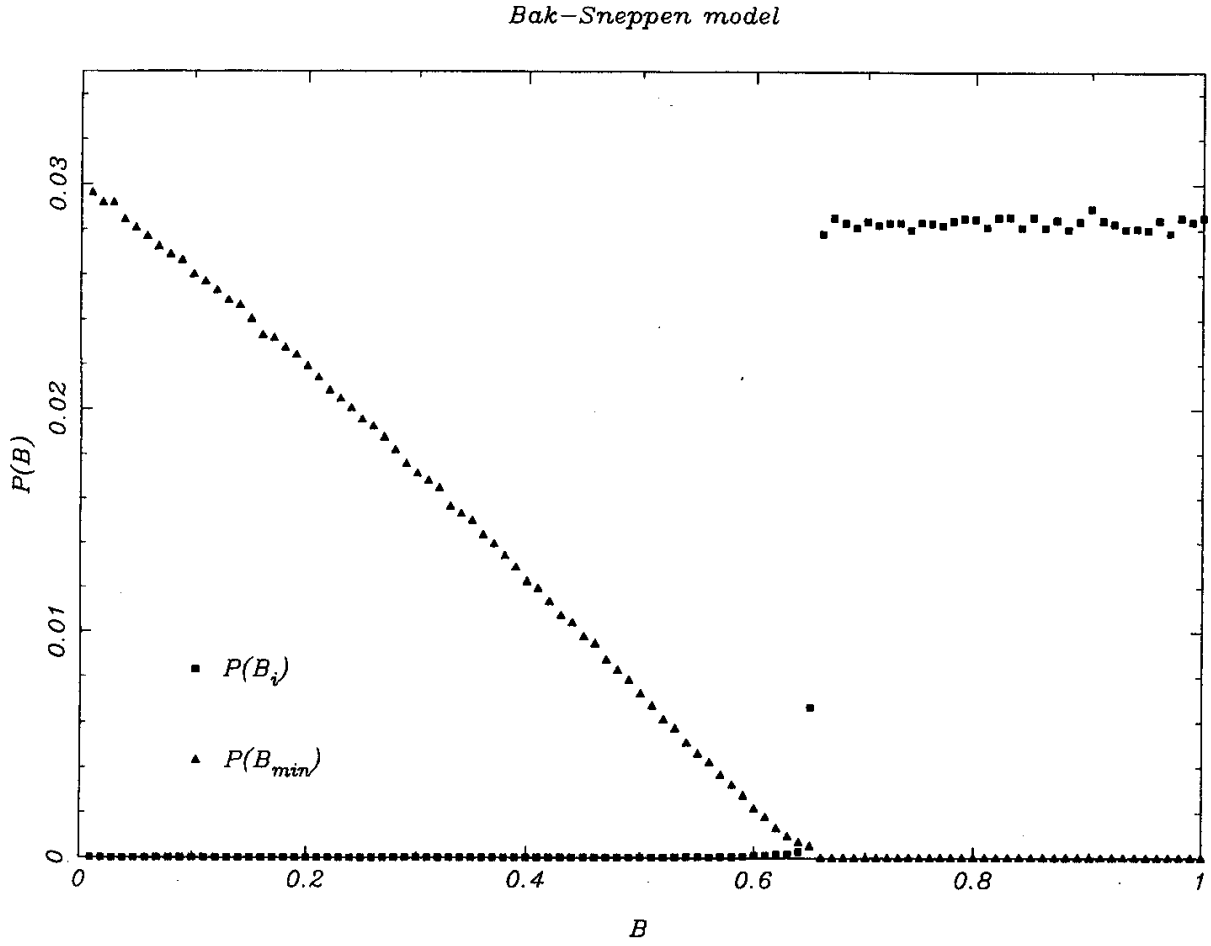

Fig. 2.5. Distributions of the barriers $P(B_i)$ (right curve) and minimum barriers $P(B_{\min})$ (left curve) in the critical state with $N = 4096$. The density of sites with random barriers B_i less than a threshold p_c vanishes, while the density above p_c is uniform. All mutations turn out to take place through barriers which are less than p_c.

of avalanche dynamics.[43] For any avalanche threshold $p < p_c$, the collection of times s, when the minimum barriers $B_{\min}(s) > p$, cut the temporal axis into a successive series of avalanches (defined by p). Therefore, on the average,

$$P(B_{\min} > p) \sim \frac{1}{\langle s \rangle_p} \sim (p_c - p)^{\gamma}, \quad \text{when} \quad p \to p_c. \tag{2.4}$$

Consequently,

$$P(B_{\min} = p) \sim (p_c - p)^{\gamma - 1}, \quad \text{when} \quad p \to p_c. \tag{2.5}$$

Figure 2.5 shows the distributions of the barriers and minimum barriers in the critical state with the system size $N = 4096$. The density of sites with random barriers B_i less than a threshold p_c vanishes, while the density above p_c is uniform. All mutations turn out to take place through barriers which are less than p_c.

It had been conjectured that the critical point p_c equals 2/3. However, by extensive numerical studies,[18] it is important to note that $p_c = 0.66702 \pm 0.00008$. This finding that p_c is not equal to 2/3 suggests that a simple analytical derivation of p_c is implausible!

3. The Critical Properties

3.1. *Fractal pattern and critical exponents*

Next, we study the statistical properties of the BS model near criticality. Figure 3.1 is a snapshot of the space-time map of activities of the BS model, in which the site with minimum barrier value at each time step is represented by a black dot. The figure indicates the space-time activity pattern of the BS model as a self-affine fractal in 1 + 1 dimensions. Jovanović *et al.*[23] have further mapped the BS model

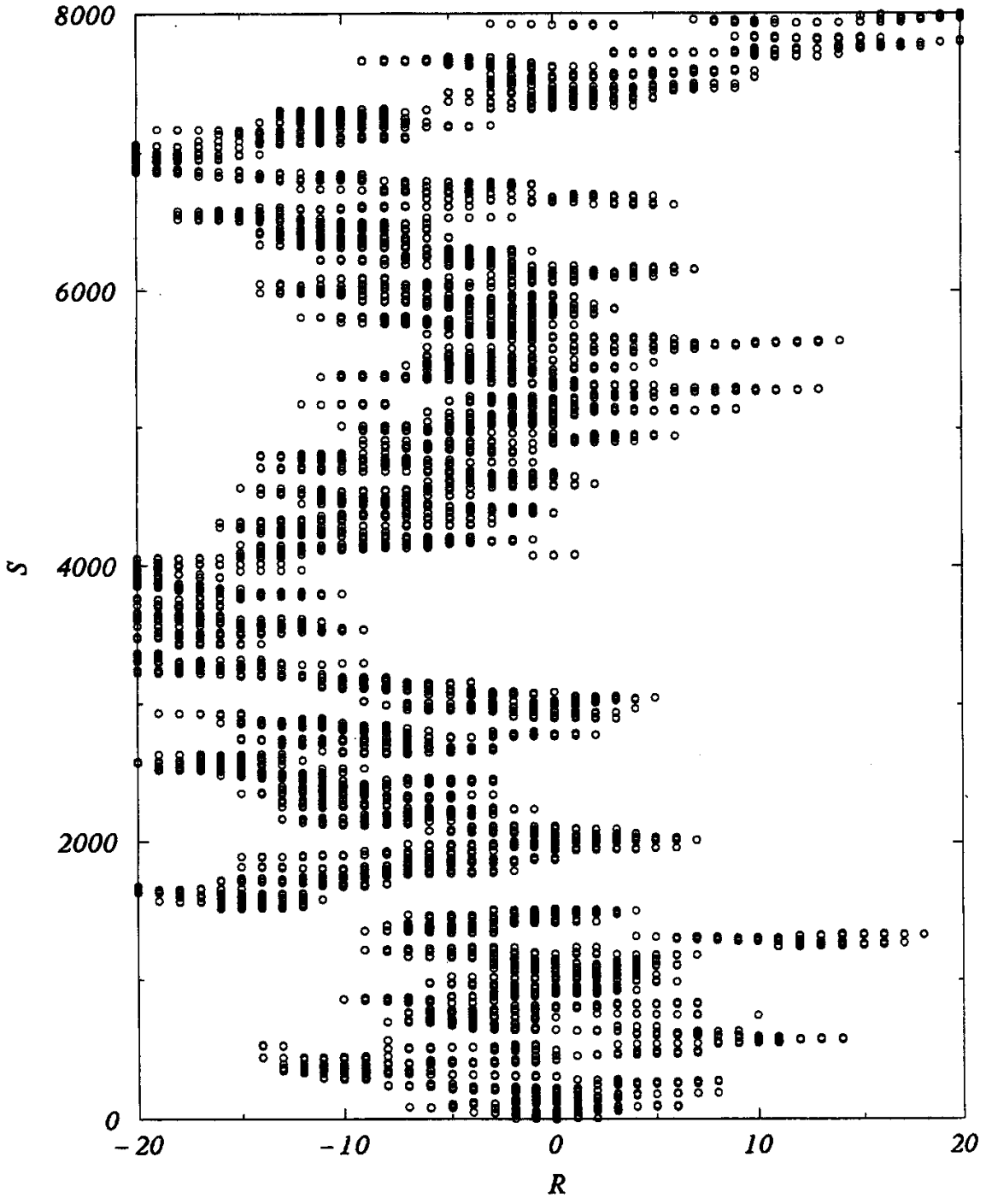

Fig. 3.1. The space-time fractal activity pattern for the BS model. Time is measured as the total number of updating.[43]

onto a "history-dependent" invasion percolation[56] type model. The scaling forms of the following properties of avalanches are in analogy with percolation.[23]

(1) The number of avalanches with size s behaves as

$$n(s) \sim s^{-\tau} f(s|p_c - p|^{1/\sigma}), \quad \text{when} \quad p \to p_c. \tag{3.1}$$

(2) The average avalanche size is

$$\langle s \rangle_p = \int n(s) s ds \sim |p_c - p|^{-\gamma}, \quad \text{with} \quad \gamma = \frac{2-\tau}{\sigma}. \tag{3.2}$$

(3) The number of avalanches with spatial extent b is

$$n(b) \sim b^{-\tau_\perp} f(b|p_c - p|^{\nu_\perp}), \quad \text{when} \quad p \to p_c. \tag{3.3}$$

(4) The average avalanche spatial extent is

$$\langle b \rangle = \int n(b) b db \sim |p_c - p|^{-\gamma_\perp}, \quad \text{with} \quad \gamma_\perp = \nu_\perp (2 - \tau_\perp). \tag{3.4}$$

From $n(s)ds = n(b)db$, we get

$$\tau_\perp - 1 = \frac{\tau - 1}{\nu_\perp \sigma}. \tag{3.5}$$

(5) A typical avalanche of size s scales with the spatial extent b as

$$s \sim b^D. \tag{3.6}$$

Since the avalanche size s is exactly equal to the number of time steps during which the avalanche lasts, so the temporal duration

$$T(= s) \sim b^D.$$

Therefore, the exponent D is not only the mass dimension relating the total amount of activities to the spatial extent, but also the dynamic exponent relating time to space. From $n(s)$ and $n(b)$, we get

$$D = \frac{1}{\sigma \nu_\perp}. \tag{3.7}$$

There are seven exponents (τ, σ, γ, $\tau_\perp$, $\sigma_\perp$, $\gamma_\perp$, D) and four relations between exponents, so there are only three independent exponents. We can choose them to be τ, $\gamma_\perp$, and D.

By the following argument, proposed by Paczuski *et al.*,[41] the value of $\gamma_\perp$ can be determined. Let us define $P(p)$ as the probability of having a p-avalanche separating

consecutive points in time where the minimum random barrier chosen is greater than p. From the definition of avalanches, we can easily get

$$P(p) \sim \frac{1}{\langle s \rangle_p} \sim (p_c - p)^{\gamma}, \quad \text{when} \quad p \to p_c. \tag{3.8}$$

An avalanche with spatial extent $\langle b \rangle_p$ leaves, on the average, $\langle b \rangle_p$ sites with new uncorrelated random barriers between p and 1. If p is increased by an infinitesimal amount dp, the number of sites with random barriers, generated by the avalanche, falling within dp of p is $\langle b \rangle_p dp/(1-p)$. Thus, the differential probability that a p-avalanche will end is derived:

$$dP(p) = \frac{dp}{1-p} \langle b \rangle_p P(p). \tag{3.9}$$

Substituting Eq. (3.8) into Eq. (3.9), we obtain

$$\gamma = \frac{\langle b \rangle_p}{1-p}(p_c - p) \quad \text{when} \quad p \to p_c. \tag{3.10}$$

Equation (3.10) is named the "Gamma Equation" by Paczuski *et al.*[41] It gives a convenient way to measure γ and p_c numerically. In plots of $(1-p)/\langle b \rangle_p$ versus p, the slope is $-1/\gamma$ and the x-axis intercept is p_c.

We can rewrite Eq. (3.10) as

$$\langle b \rangle_p = \gamma \frac{(1-p)}{(p_c - p)} = \gamma \frac{(1-p_c) + (p_c - p)}{(p_c - p)}.$$

Then,

$$\langle b \rangle_p \sim (p_c - p)^{-1}, \quad \text{when} \quad p \to p_c.$$

Therefore, the value of $\gamma_\perp$ is obtained as

$$\gamma_\perp = 1. \tag{3.11}$$

Consequently, there remain only two independent exponents D and τ, the fractal exponent of the avalanches and the avalanche size distribution exponent, respectively.

There have been a few numerical attempts[18,23,42,43] not only for pinning down the values of exponents τ and D, but also for verifying the dynamical scaling hypothesis on the geometrical properties of avalanches. For computational efficiency, the "BS branching process", proposed by Paczuski *et al.*,[42] is simulated to obtain the information regarding the critical properties of avalanches. The algorithm of the "BS branching process" is as follows. It starts with a single site with barrier value p, which defines the avalanche threshold. Then random numbers are given to this site and its nearest neighbors. Only the random numbers smaller than the avalanche threshold p are stored along with their positions. At next time step, the one with

the minimal number is selected and the new random numbers are given to it and its nearest neighbors. The process continues until there are no more stored random numbers. When p is very close to p_c, the mean avalanche size becomes extremely large. Therefore, it is essential to cut the process off at some maximal time T. This algorithm leads to exactly the same distribution of avalanches as the original BS model. The control parameter p plays the role of the avalanche threshold. From the computational point of view, the "BS branching process" is most rapid and it excludes the finite site effect.

Table 1 gives the values of critical exponents of avalanches measured by several groups.[23,18,43] The reader can check that all these exponents are consistent, within

Table 1. The numerically measured values of critical exponents and their associated uncertainties in the BS model. ( ) indicates uncertainty in the last digit. The data, from top to bottom, are taken from Refs. 18, 23 and 43, respectively.

D	τ	γ	$\gamma_\perp$	σ	$\nu_\perp$
2.33(5)	1.08(5)	2.7(1)	0.98(3)	0.35(2)	1.23(8)
2.43(1)	1.073(3)	2.70(2)	—	0.346(5)	—
2.43(1)	1.07(1)	2.70(1)	—	—	—

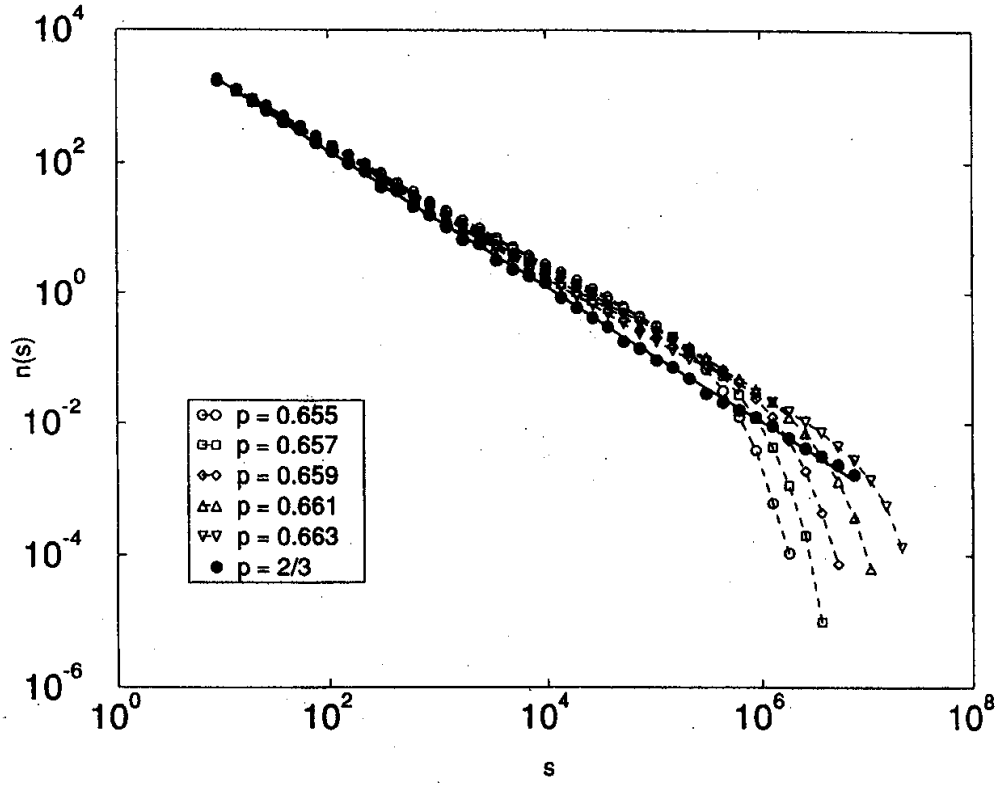

Fig. 3.2. The distribution of avalanches $n(s)$ as a function of s, on the logarithmic scale, for different values of avalanche threshold $p \leq p_c$.[23]

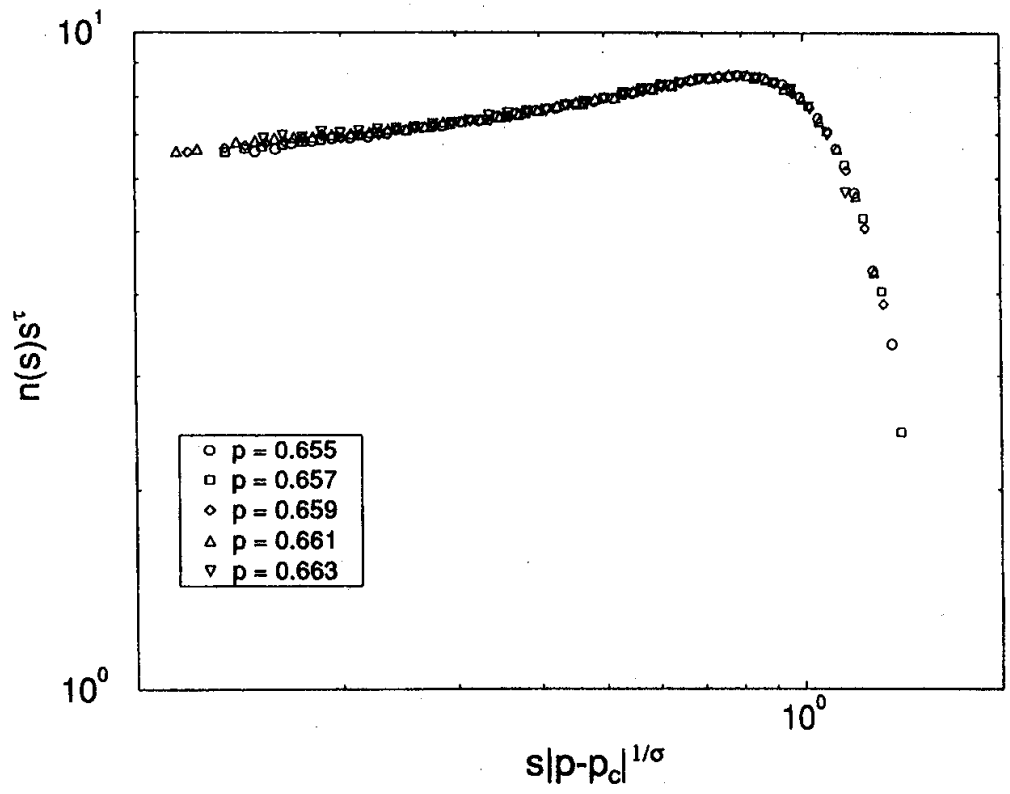

Fig. 3.3. The scaling plot of $n(s)$, i.e. $n(s)s^{\tau}$ versus $s|p_c - p|^{1/\sigma}$ on a logarithmic scale, using $\tau = 1.08 \pm 0.05$ and $\sigma = 0.35 \pm 0.02$.[23]

the uncertainties of numerical measurement, with the exponent relations [Eqs. (3.2), (3.4), (3.5), (3.7) and (3.11)] based on the dynamic scaling hypothesis. Figure 3.2 shows the distribution of avalanches $n(s)$ as a function of s, on the logarithmic scale, for different values of avalanche threshold $p \leq p_c$.[23] Figure 3.3 is the scaling plot of $n(s)$, i.e. $n(s)s^{\tau}$ versus $s|p_c - p|^{1/\sigma}$ on a logarithmic scale, using $\tau = 1.08 \pm 0.05$ and $\sigma = 0.35 \pm 0.02$.[23] The excellent data collapse strongly affirms the dynamic scaling assumption regarding the geometric properties of avalanches near the critical point p_c.

3.2. *Spatial-temporal correlation*

In this section, we focus on the spatial-temporal correlation between successive evolution events. It is straightforward to see that, in the beginning, subsequent activities in the system are quite uncorrelated in space. But the correlation between activities is gradually developed as the gap $p_{\min}(s)$ increases, since it becomes more likely that near neighbors of the previous minimal site are next to be activated. After an extensive transient period, the distribution of correlation becomes stationary.

$P(x, \Delta s)$ is defined as the probability distribution of distance x between sites of subsequent activity which occurs after a time Δs. During an avalanche all $B_{\min}(s) < p$ are taken from these newly appeared barriers. Thus, the $B_{\min}(s)$ are randomly distributed in space; i.e. the distance between successive activities is also equally

distributed as long as the distance x is less than the avalanche spatial extent $\langle b \rangle_p$. In addition, the normalization condition requires $\int P(x, \Delta s)dx = 1$. Thus, we can write $P(x, \Delta s)$ in the following scaling form

$$P(x, \Delta s) = \frac{1}{\Delta s^{1/D}} f\left(\frac{x}{\Delta s^{1/D}}\right),$$

where

$$f(y) = \begin{cases} \text{constant} & y \ll 1 \\ y^{-\pi} & y \gg 1. \end{cases} \tag{3.12}$$

By scaling analysis,[31,33,40] the exponent π can be expressed as

$$\pi = 1 + (2 - \tau)D. \tag{3.13}$$

Numerical studies[40] have affirmed explicitly the prediction[31] of the dynamic scaling form of the spatial-temporal correlation between successive evolution events. Figure 3.4 is the log–log plot of $P(x, \Delta s)$ versus x.[40] Curves with a larger Δs have

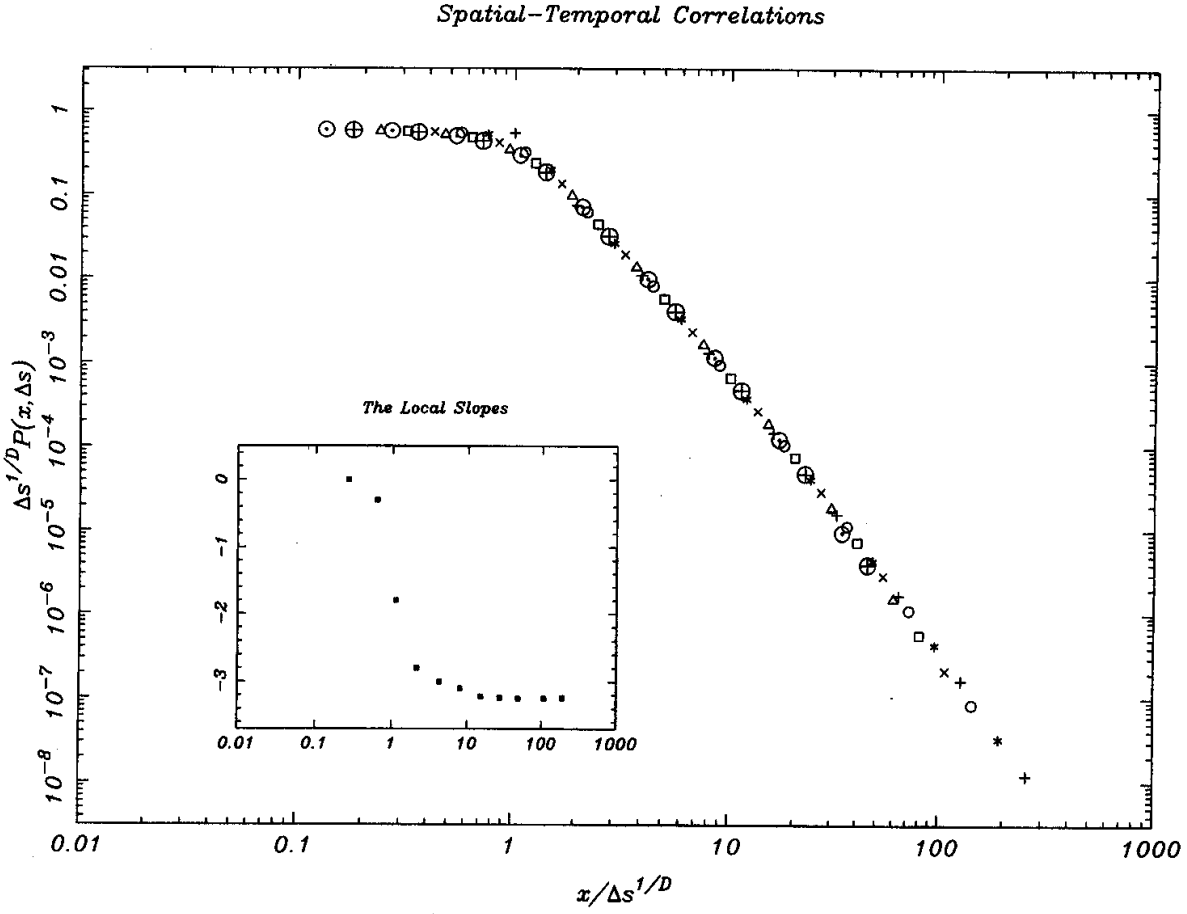

Fig. 3.4. Logarithmically binned distribution of distances x between subsequent activities which occur after a time interval $\Delta s = 1, 2, 4, \ldots, 128$. $P(x, \Delta s)$ is the density of x in the range $[x, 2x)$. Curves with a larger Δs have a wider plateau.[40]

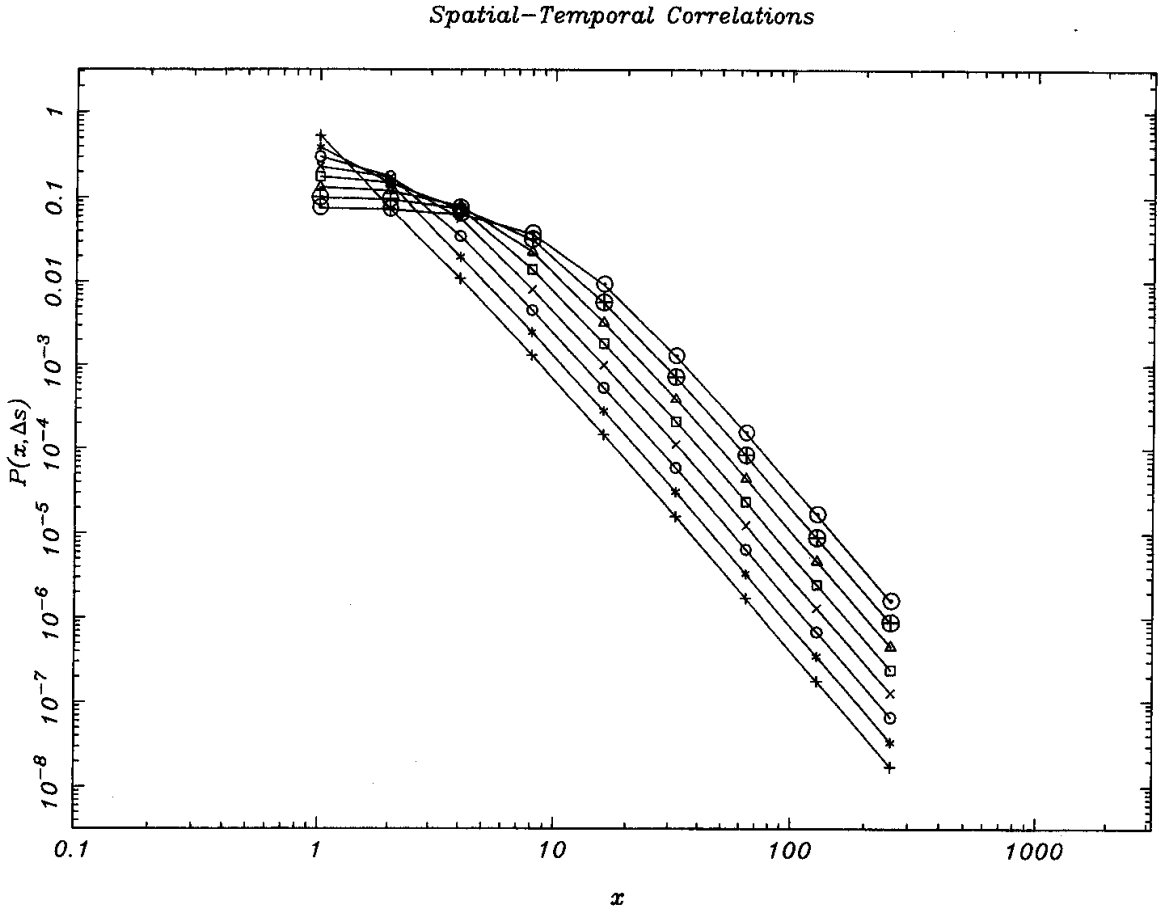

Fig. 3.5. The scaling plot of the distribution $P(x, \Delta s)$, i.e. $\Delta s^{1/D} P(x, \Delta s)$ versus $x/(\Delta s^{1/D})$ on a logarithmic scale,[40] using $D = 2.43 \pm 0.01$. By extrapolating the local slopes to the power-law decay of $P(x, \Delta s)$ (see the insert), the exponent π is obtained as 3.24 ± 0.02, in agreement with the scaling relation $\pi = 1 + (2 - \tau)D$, based on the exponents $D = 2.43 \pm 0.01$ and $\tau = 1.073 \pm 0.003$ in Refs. 18 and 43.

a wider plateau. Figure 3.5 is the scaling plot of $P(x, \Delta s)$, i.e. $\Delta s^{1/D} P(x, \Delta s)$ versus $x/(\Delta s^{1/D})$ on a logarithmic scale,[40] using $D = 2.43 \pm 0.01$. By extrapolating the local slopes to the power-law decay of $P(x, \Delta s)$ (see the insert of Fig. 3.5), the exponent π is obtained as 3.24 ± 0.02, in agreement with the scaling relation $\pi = 1 + D(2 - \tau)$, based on the exponents $D = 2.43 \pm 0.01$ and $\tau = 1.073 \pm 0.003$ in Refs. 18 and 43.

Subsequently, the spatial correlation function $P_x(x)$, the probability that the minimal sites at two successive updates are separated by x sites, is by definition equal to $P(x, \Delta s = 1)$ and, therefore,

$$P_x(x) \equiv P(x, \Delta s = 1) \sim x^{-\pi}, \quad \text{with} \quad \pi = 3.24 \pm 0.02. \tag{3.14}$$

We see that the spatial correlation function $P_x(x)$ is somewhat similar to the usual one-dimensional Lévy flight random walk,[53] where at each time step the walker jumps by a distance drawn from a power-law distribution. However, the activities in the BS model are also temporally correlated, in contrast to the temporally

uncorrelated nature of the Lévy flight random walk.[53] The temporal correlation function $P_t(\Delta s)$ is defined as the probability that a given site, being the minimal site at time s_0, will again be the minimal site at time $s_0 + \Delta s$ regardless of what happens at intermediate times. By definition,

$$P_t(\Delta s) \equiv P(x = 0, \Delta s) \sim \Delta s^{-1/D}, \quad \text{with} \quad D = 2.43 \pm 0.01. \tag{3.15}$$

The numerical confirmation of the scaling forms of $P_x(x)$ and $P_t(\Delta s)$ is given in Refs. 9 and 43. It is important to note that the spatial and temporal correlation functions, $P_x(x)$ and $P_t(\Delta s)$, are two of the main qualitative differences between the BS model and its random neighbor variant, which will be discussed in the next section.

Maslov *et al.*[35] have pointed out that the power spectrum of the system is simply

$$S(f) = \int d(\Delta s) P_t(\Delta s) \exp(2\pi i f \Delta s) \sim \frac{1}{f^{1-1/D}}. \tag{3.16}$$

Therefore, $1/f$ type noise emerges naturally as a result of avalanche dynamics. We see that the exponent $\tilde{d}$ that characterizes $1/f$ type noise is equal to $1 - 1/D$ and, consequently, a formal relation between $1/f$ type noise and fractal spatial behavior is established[35] through the fractal exponent D of avalanches. The numerical confirmation is shown in Fig. 3.6, which is the log–log plot of power spectrum $S(f)$

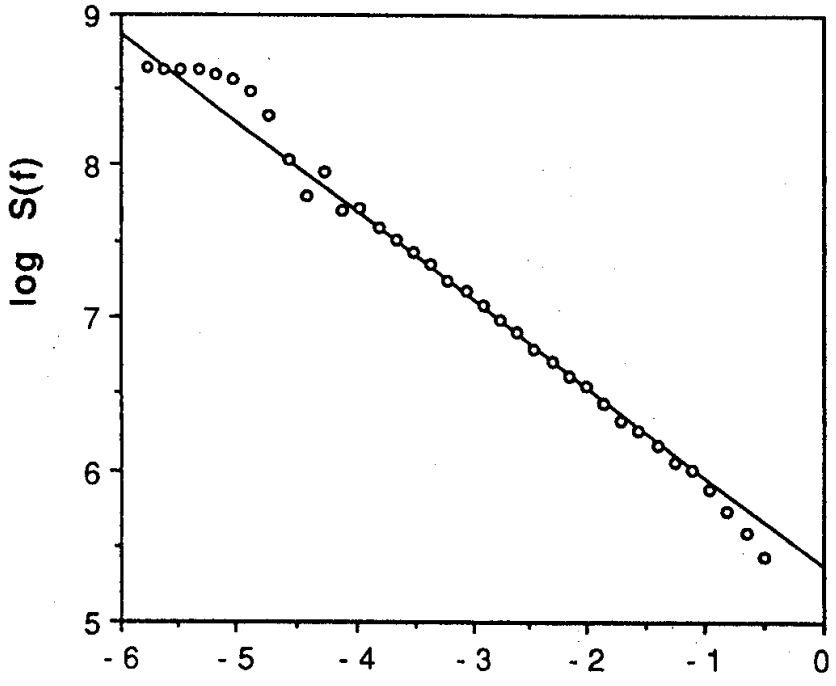

Fig. 3.6. The log-log plot of power spectrum $S(f)$ versus frequency f.[43] The straight line, obtained from the least squares fit to the data, gives the exponent $\tilde{d}$ equal to 0.58, in agreement with the scaling relation $\tilde{d} = 1 - 1/D$, based on the exponent $D = 2.43 \pm 0.01$ in Refs. 18 and 43.

versus frequency f.[43] The straight line, obtained from the least squares fit to the data, gives the exponent $\tilde{d}$ equal to 0.58, in agreement with the scaling relation $\tilde{d} = 1 - 1/D$, based on the exponent $D = 2.43 \pm 0.01$ in Refs. 18 and 43.

Note that, at any given site, the activity is recurrent in time as a "fractal renewal process".[43,29] The first return probability $P_{\text{first}}(\Delta s)$ is defined as the probability that a given site, being the minimal site at time s_0, will again be the minimal site *for the first time* at time $s_0 + \Delta s$. The time interval Δs separating subsequent recurrence of activities at any given site could be viewed as an analogy of the stochastic *waiting time* in the surface growth models.[54] Maslov *et al.*[35] have obtained the first return probability distribution as

$$P_{\text{first}}(\Delta s) \sim \Delta s^{1/D-2}, \quad \text{for} \quad \Delta s \gg 1, \tag{3.17}$$

and numerically confirmed their prediction. The power-law behavior of the first return probability distribution is also a manifestation of the existence of $1/f$ type noise.[29] Consequently, all the exponents characterize the spatial-temporal correlation of the system can be expressed in terms of D and τ, the fractal exponent of the avalanches and the avalanche size distribution exponent, respectively.

4. The Random Neighbor Variant

4.1. *The mean field approach*

Since most results in the BS model can only be obtained by either scaling analysis or numerical simulation, it behooves us to look at the random neighbor variant,[17] which is the first step towards a solvable mean field treatment.[17,47] In addition, exact or rigorous results of the random neighbor variant can be obtained in the thermodynamic limit, i.e. the system size $N \to \infty$.[7,9]

The random neighbor variant is defined as follows. Initially, the random numbers B_i, drawn independently from a uniform distribution $[0, 1]$, are assigned to each site i of a one-dimensional line, $i = 1, \ldots, N$, with periodic boundary conditions. Then, the updating rule is that, at each time step, new barriers are assigned to *the minimal site* and *two additional sites chosen at random* . These new random numbers are also drawn independently from a uniform distribution $[0, 1]$. In the following, I will first give some intuitive arguments. Then, the main scheme and simple derivations of the mean field treatment will be reviewed.

It has been mentioned in the previous sections that the gap $p_{\min}(s)$, defined as the largest of the minimal $B_{\min}$ which have been selected up to time s, is an increasing function of time. Suppose, at time s_0, the gap $p_{\min}(s_0)$ reaches the value $1/3$, thus the smallest barrier is equal to $1/3$ and the other $N - 1$ barrier values are larger than $1/3$. The updating process, assigning new random numbers to *the minimal site* and *two additional sites chosen at random*, results in again one barrier value below $1/3$ and the other $N - 1$ barriers larger than $1/3$, on the average. Consequently, we see that the gap $p_{\min}(s)$ reaches its stationary state at time s_0. It is obvious to tell that the critical threshold p_c is $1/3$ and, on the average, there is

only one site with the random number below the threshold p_c in the thermodynamic limit. Thus, we expect that the distribution of barrier values vanishes below p_c and is a constant above p_c, while the distribution of minimum barrier vanishes above p_c and is a constant below p_c.

As usual, the mean field theory[17,9] can be constructed by neglecting correlations between barrier values. Namely, the joint probability distribution $P(B_1, \ldots, B_N; s)$ of barrier heights is replaced by the average distribution $P^N(B, s)$, where N is the system size. With the definition $Q(B, s) \equiv \int_b^1 P(B, s) dB$, it is evidently

$$P(B, s) = -\frac{dQ(B, s)}{dB} \tag{4.1}$$

and

$$P(B_{\min}, s) = -\frac{dQ^N(B, s)}{dB}. \tag{4.2}$$

The master equation for $P(B, s)$ is simply

$$\begin{aligned} P(B, s+1) =& P(B, s) - \frac{1}{N} P(B_{\min}, s) \\ & - \frac{2}{N-1}\left(P(B, s) - \frac{1}{N} P(B_{\min}, s)\right) + \frac{3}{N}. \end{aligned} \tag{4.3}$$

On the right-hand side of Eq. (4.3), the last three terms represent the removal of the minimum barrier, the removal of two barriers from the other $N-1$ barriers, and the addition of three new equidistributed barrier values, respectively. By demanding $P(B, s+1) = P(B, s)$ for the stationary state, a simple relation for the equilibrium distribution $Q(B)$ is obtained

$$(N-3)Q^N(B) + 2NQ(B) + 3(N-1)(B-1) = 0. \tag{4.4}$$

By numerically solving Eq. (4.3) and applying Eqs. (4.1) and (4.2), the numerical values for $P(B)$ and $P(B_{\min})$ for all values of barrier heights can be obtained.[17,9] In the limit $N \to \infty$, the average equilibrium distribution of barrier heights is

$$P(B) \simeq \begin{cases} 0, & B \ll 1/3 \\ 3/2, & B \gg 1/3 \end{cases} \tag{4.5}$$

and the equilibrium distribution of minimum barrier is

$$P(B_{\min}) \simeq \begin{cases} 3, & B \ll 1/3 \\ 0, & B \gg 1/3. \end{cases} \tag{4.6}$$

This result is consistent with the intuitive expectation.

Flyvbjerg *et al.*[17] have pointed out that, in the mean field approximation, an avalanche in the random neighbor variant can be identified as a critical branching process with branching ratio 3.[20] Therefore, the distribution of avalanche size is

$$n(s) \sim s^{-3/2},$$

as that in the critical branching process. This prediction has been numerically confirmed.[7]

However, note that the usual assumption of mean field theory is that fluctuations of quantities are small compared to their average value in the thermodynamic limit. When the fluctuation of a quantity is of the same order as its average value, the mean field theory is not suitable for describing such a quantity. Therefore, as pointed out in Ref. 9, mean field theory fails to describe the distribution of active sites, i.e. the sites with barrier values less than p_c, the distribution of minimum barriers near criticality, etc. This point will be discussed further in the following.

4.2. *Exact results beyond mean field*

The mapping of self-organized critical models to a one-dimensional random walk problem[24,2,7] has been a useful tool in obtaining information related to the avalanche dynamics of the system. An avalanche can be thought as a directed random walk on the non-negative integers, starting from zero and terminating when it returns to zero again for the first time. The main merit of this formalism is to give the insight on the generation of power-law distribution and other properties of one given avalanche; however, it is not suitable for describing correlations between different avalanches, unless a more complicated interacting random walk formalism is introduced.[24] Note that through the use of random walk techniques, exact or rigorous results of the random neighbor variant can be obtained in the thermodynamic limit, i.e. the system size $N \to \infty$.[7,9] In the following, I will give a brief review about its main scheme, which is applicable to other self-organized critical models.

First, $N_{\rm act}(s)$ is defined as the number of active sites at any given time s. An active site is any site of which the barrier height is less than the avalanche threshold p. An avalanche of size $\tilde{s}$ starts when the number of active sites $N_{\rm act}(s)$ changes from zero to a positive integer at time s_0 and ends when $N_{\rm act}(s)$ is again zero for the first time at time step $s_0 + \tilde{s}$. The update rule for changing the number of active sites can be viewed as the random walk rule specifying the random walk of $N_{\rm act}(s)$. Since, besides the minimal site, the location of two additional sites for updating is chosen at random, there is no spatial correlation between different sites. Thus, it is easy to write down the updating rule for the random walk of $N_{\rm act}(s)$ as follows.[9] The probability of reducing the number of active site by r, through the removal of the minimal site and two other additional sites chosen at random, is given as

$$P_{\rm dec}(r) = \frac{C_{r-1}^{N_{\rm act}-1} C_{3-r}^{N-N_{\rm act}}}{C_2^{N_{\rm act}-1}}. \tag{4.7}$$

The probability of increasing the number of active sites by m, through assigning new random numbers to these sites is given as

$$P_{\text{inc}}(m) = C_m^3 p^m (1-p)^{3-m}. \tag{4.8}$$

Note that the knowledge of P_{dec} and P_{inc} enables us to obtain almost all the properties regarding avalanches. In contrast, for the original BS model, it is difficult to write down P_{dec} due to the strong spatial correlation of the system and, therefore, indicates why the BS model is more stubborn analytically.

As mentioned in the previous section, the mean field theory is suitable to describe the quantities of which the fluctuations are small compared to their averages. Indeed, we see that the exact result of the distribution of avalanche size in the thermodynamic limit is

$$n(s) = \sqrt{\frac{3}{4\pi}}\, s^{-3/2} + O(s^{-5/2}),$$

which is consistent with the mean field approach. It is interesting to note that the same-site first return probability $P_{\text{first}}(\Delta s)$, i.e. the minimal site being again the minimal *for the first time* at time Δs later, can be obtained exactly, through the use of the active site formalism,[9]

$$P_{\text{first}}(\Delta s) = \frac{2}{9\sqrt{3\pi}}\, \Delta s^{-3/2} + O(\Delta s^{-5/2}). \tag{4.9}$$

This result is consistent with the intuitive picture of the random neighbor variant: the minimal site performs a modified directed random walk in the space-time plot!

However, if the fluctuation of a quantity is of the same order as its average value, the mean field theory fails to describe such a quantity. For example, the exact result, by using the random walk techniques,[9] of the average number of active sites in the equilibrium state is

$$\langle N_{\text{act}} \rangle \equiv \sum P(N_{\text{act}}) N_{\text{act}} = \frac{3p(1-2p)}{(1-3p)} \tag{4.10}$$

and its standard deviation is

$$\delta N_{\text{act}} = \frac{\sqrt{3p}}{1-3p}\left(1 - 6p + \frac{38}{3}p^2 - 8p^3\right)^{1/2}. \tag{4.11}$$

Clearly, we see that

$$\delta N_{\text{act}} > \langle N_{\text{act}} \rangle \quad \text{for all } p < p_c$$

and

$$\delta N_{\rm act} = \langle N_{\rm act} \rangle \quad \text{for } p = p_{\rm c}.$$

In contrast, the mean field result is

$$\langle N_{\rm act} \rangle = -\log(1 - 3p), \tag{4.12}$$

which deviates from the exact result for all $p < p_{\rm c}$.

Moreover, the rigorous result, through the use of the active site formalism, of the distribution of minimum barrier $P(B_{\rm min})$ near criticality is also different from the mean field result. Since the region near criticality is most relevant to the avalanche dynamics, this discrepancy of the mean field result from the rigorous result is a significant evidence for the shortcomings of the mean field treatment. Ref. 9 gives a very thorough table of $P(B_{\rm min})$, for the comparison between the numerical simulation of the random neighbor variant, the mean field result, and the rigorous result derived from the active site formalism.

4.3. *Important differences from the BS model*

The random neighbor variant does possess some properties qualitatively identical to those of the BS model. For example, it also has nontrivial distributions of barrier heights and minimum barriers, and a power-law avalanche size distribution.[17,9] The original motivation for the random neighbor variant is that it is easy to solve and allows for the straightforward mean field approach. However, this simplification process has sort of dangerous potential to wash out some important and salient features of the original model. The key differences between these two models are listed as follows.

First of all, de Boer *et al.*[9] have pointed out that the spatial correlations of the random neighbor variant are significantly different from those in the original BS model. From the definition of the random neighbor variant, we see that there is no spatial correlation except the same-site correlation of the minimal site. That is, spatial correlations have been degraded from *power laws* to *a δ-function.* Thus, in contrast to the original BS model, where sites with barrier values larger than $p_{\rm c}$ can be reactivated again and again through long-range spatial correlation, any given site in the random neighbor variant can be active only for a finite number of times. Moreover, the same-site temporal correlation function, i.e., the minimal site being again the minimal at time Δs later, $P_t^{\rm RN}(\Delta s)$ in the random neighbor variant behaves as

$$P_t^{\rm RN}(\Delta s) \sim \Delta s^{-3/2}. \tag{4.13}$$

Consequently, $P_t^{\rm RN}(\Delta s)$ is normalizable; namely, *the sum over $P_t^{\rm RN}(\Delta s)$ converges.* Remember that, in Sec. 3, the original BS model has

$$P_t^{\rm BS}(\Delta s) \sim \Delta s^{-1/D}, \quad \text{with} \quad D = 2.43 \pm 0.01,$$

so that *the sum over $P_t^{\rm BS}(\Delta s)$ diverges*!

In addition to the differences listed above, in the original Bak–Sneppen model, the sites with small values of B_i have the tendency to be clustered together. Flyvbjerg *et al.*[17] have shown numerically that the BS model is better approximated by updating *the two sites with the smallest and the second smallest values plus one randomly selected site.* Consequently, the critical threshold p_c is close to 2/3 instead of 1/3, the value of p_c in the random neighbor variant, and the distribution of minimum barrier has *power-law behavior* below p_c, in contrast to being almost *a step function* in the random neighbor variant.

Because of the connected nature of the set of active sites, any given avalanche in the original BS model is characterized by its size s and spatial extent b. The fractal nature of avalanches is manifest through the relation

$$s \sim b^D, \quad \text{with} \quad D = 2.43 \pm 0.01.$$

Clearly, by virtue of the definition of the model, *the possibility of a connected nature of avalanches is simply absent in the random neighbor variant.* Therefore, any exponent related to the spatial extent of avalanches, such as $\tau_\perp$, $\nu_\perp$, $\gamma_\perp$, and D, has no physical meaning in the random neighbor variant.

5. Relation with Other Problems

5.1. *Directed percolation*

Recall that the definition of directed percolation is the same as that of ordinary percolation but assigning directions to each bond[21] (see Fig. 5.1 for illustration). In Fig. 5.1, the direction of the arrow on each bond gives the passage direction.

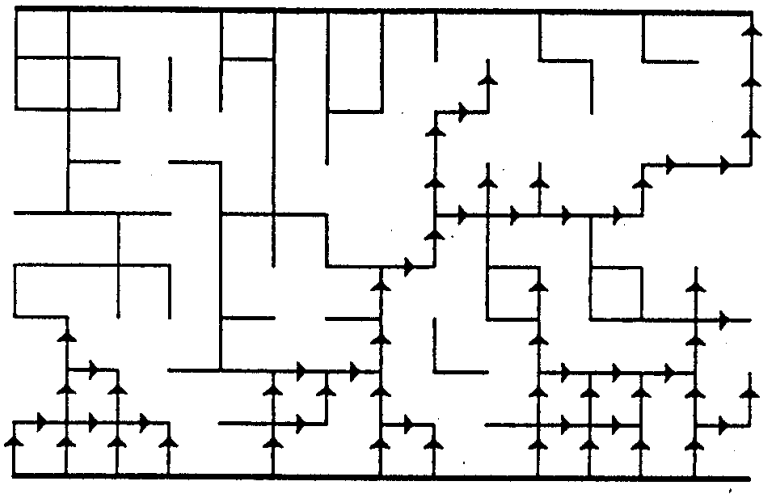

Fig. 5.1. The illustration of $1+1$-dimensional bond directed percolation on a square lattice.[21] The direction of the arrow on each bond gives the passage direction. We see that vertical bonds point in the positive y direction and horizontal bonds point in the positive x direction. Therefore, the vector $(x = 1, y = 1)$ can be labeled as the direction of time. Percolation is only allowed in the direction of increasing time.

We see that vertical bonds point in the positive y direction and horizontal bonds point in the positive x direction. Therefore, the vector $(x = 1, y = 1)$ can be labeled as the direction of time. Percolation is only allowed in the direction of increasing time. Due to the similarity in model definition to some extent, Ray and Jan[47] first proposed the conjecture that the BS model is in the directed percolation (DP) universality class. Since then, there has been much debate[18,23,42,47] regarding this conjecture.

By redefining the time variable in the BS model as $t \to t + 1/N_{\text{act}}(s)$ for each sequential update of the system, Paczuski *et al.*[42] argued that BS model is in the same universality class of directed percolation (DP), described by Reggeon Field Theory (RFT). The scheme of their argument is as follows: (1) Assume that the random numbers of active sites (inside an avalanche) are annealed at each time step. In contrast, in the BS model, these random numbers are quenched. (2) The annealed case belongs to the university class of RFT. (3) They argued that the updating order is not important. Therefore, the quenched case (BS) also belongs to the same university class.

Intuitively, the above argument seems plausible at the first glance. However, as mentioned in the previous section, the sites with small values of B_i in the BS model have the tendency to be clustered together. The annealed case certainly loses this property. Thus, the spatial extext of the annealed case is wider than that of the original BS model, because the sites in the edge have the equal opportunity to be updated. The question is then whether this difference will influence the values of the exponents or just the prefactors.

Jovanović *et al.*[23] checked the validity of the above claim by numerical simulation. In their paper Model 1, in which the column with the smallest barrier is selected, corresponds to the BS model. Model 3, in which the column for updating is selected randomly among those with barriers smaller than p, corresponds to the annealed case. Their simulation result shows that the updating order is important. Model 3 has the same behavior as DP (directed percolation), i.e., the same scaling indices. The numerically measured values of critical exponents in Model 3 and those in DP are listed in Table 2. In contrast, the exponents which characterize the scaling of the variables with $|p_c - p|$ are different for Model 1 and for DP. The numerically measured values of critical exponents in Model 1 are listed in Table 1.

Table 2. The numerically measured values of critical exponents and their associated uncertainties in Model 3 of Ref. 23 and $1 + 1$ dimensional directed percolation (DP), also taken from Ref. 23. ( ) indicates uncertainty in the last digit.

	D	τ	γ	$\gamma_\perp$	σ	$\nu_\perp$
Model 3	2.33(5)	1.08(5)	2.3(1)	0.83(2)	0.40(2)	1.11(8)
DP	2.33	1.12	2.28	0.82	0.39	1.097

Finally, by extensive simulation, Grassberger[18] gives $\gamma = 2.70 \pm 0.02$, reconfirming the measurement of Jovanović *et al.*[23] Moreover, Grassberger's[18] measurement, $D = 2.43 \pm 0.01$, even ruled out the possibility that the exponents characterizing the relation between the geometric variables of avalanches are the same for the BS model and DP.

However, the discrepancy between the numerical values of the critical exponents in the BS model and those of DP is somewhat moderate. People might argue that this is due to the statistical deviation, finite size effects, or slow crossover behavior, etc. Therefore, a rigorous argument proving (or disproving) this conjecture is very much needed for resolving this controversy.

5.2. *Related models of self-organized criticality*

The concept of self-organized criticality was introduced by Bak, Tang, and Wiesenfeld[12,13] to describe certain large dynamical systems in which criticality arises without fine tuning of any external parameter. The paradigmatic example of a self-organized critical system is the abelian sandpile model.[12,13] By studying avalanche dynamics in piles of rice, Frette *et al.*[14] recently have given some experimental verification for the theoretical prediction of the sandpile model.

Unlike the sandpile model consisting of the local conservation law, the BS model is characterized by the globally extremal dynamics. It shares some similarity with self-organized interface depinning (SOID) models.[1,30,38,39,51] Especially, it can be regarded as the baby version of the invasion percolation model.[56] A very thorough and pedagogical review is given in Ref. 43. Here, I will briefly mention the most salient features shared by these models and the subtle differences between them.

The updating rules of these SOID models all involve the globally searching for the minimal site. The differences between them are the surface relaxation rules after picking up the minimal site. One of the most well-known SOID models is the Sneppen model, which represents the advance of a fluid through a piece of paper.[3,5] In the Sneppen model, the surface relaxation rule is to advance all the neighboring sites until the interface satisfies the restricted solid-on-solid (RSOS) condition, i.e., the local slopes of the interface being 1, 0, or -1. This model is equivalent to the KPZ (Kardar–Parisi–Zhang) model[28] with quenched noise, of which the scaling exponents can be obtained[1,30,39] by mapping the interface to the directed percolating path.

As pointed out in Ref. 39, there are two main features in these SOID models: (i) *the blocking surfaces* and (ii) *the avalanche dynamics. The blocking surfaces* refer to the tendency of any interface segment remaining stationary for a long period at some metastable state until failing to adapt to the changing neighboring landscape, and then moving forward rapidly until being pinned at some metastable state again. The scaling forms of *the avalanche dynamics* are similar to those defined in the BS model. Based on the geometric compactness of the avalanches and the nonexistence of multifractal scaling in the system, we can easily write

$$r_{\|}^{D} \sim s \sim r_{\perp} r_{\|} \sim r_{\|}^{\chi} r_{\|} \sim r_{\|}^{1+\chi},$$

where s is the avalanche size, $r_{\|}$ is the avalanche width parallel to the substrate, and $r_{\perp}$ is the avalanche width perpendicular to the substrate. Thus, the usual interfacial saturated roughness exponent χ, which characterizes the critical growing interface, is related to the fractal exponent of the avalanches D via

$$D = 1 + \chi. \tag{5.1}$$

Through the formalism in Ref. 23, the BS model, being coined the term "history-dependent invasion percolation type model",[23] can be viewed as the advance of interface in spatial-time plot *without any kind of surface relaxation.*

The invasion percolation[56] model has exactly the same updating rule as the BS model except it is a quasi-2-dimensional, instead of $1+1$-dimensional, model. This model is defined as follows. Random numbers, drawn independently from the uniform distribution, are assigned to each site on a 2-dimensional lattice of linear size N. Initially, the "invading fluid" occupies the left edge of the lattice, with periodic boundary conditions on the top and bottom edges. At each update, the site with the smallest random number among all the perimeter sites is occupied by the "invading fluid". The process continues until the "invading fluid" reaches the right edge of the lattice. Note that *the universality class of this model is very sensitive to the definition of perimeter sites.*[43] In Ref. 15, the authors have observed the *intermittent behavior* of the advance of the interface (see Fig. 5.2 for illustration). Figure 5.2 shows that the pattern of activity in invasion percolation looks like a fractal, which has been numerically verified.[56]

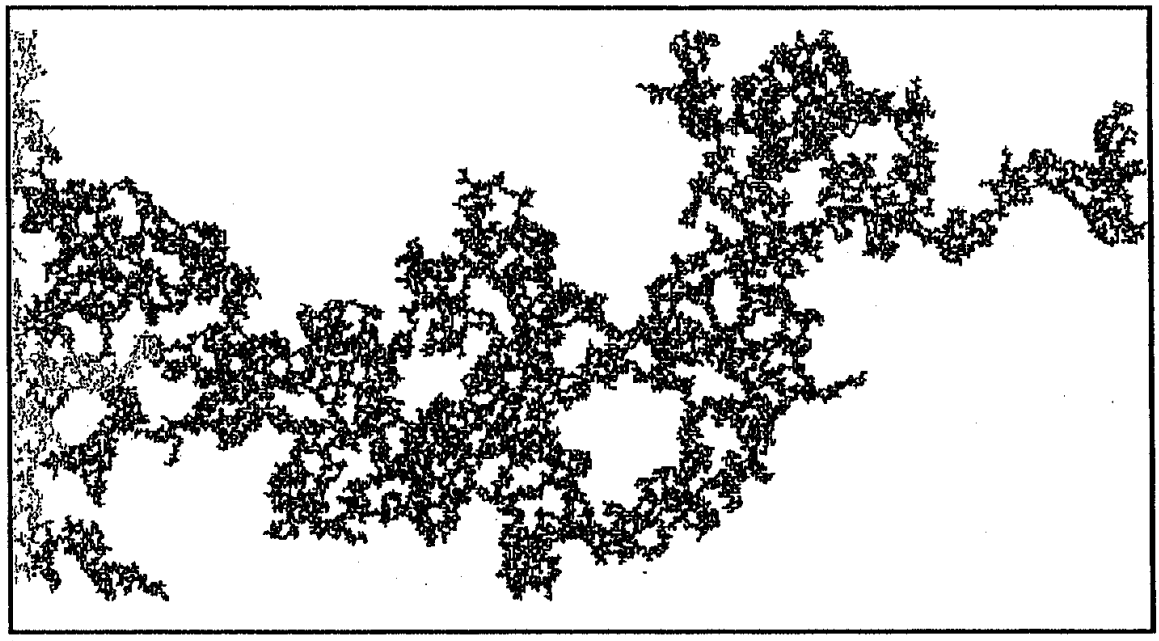

Fig. 5.2. The illustration of site invasion percolation on a square lattice with trapping.[15]

Roux and Guyon[46] first used the language of avalanche dynamics to study this model. The system does show the characteristic of the self-organized critical behavior, e.g. the existence of some critical threshold p_c, the power-law behavior of spatial-temporal correlation, the fractal pattern of activities, etc. Note that, in all the analytical and numerical treatments,[15,43,46,56] the system is assumed to be isotropic, based on the updating rule being without directional preference. However, this assumption is questionable, since the initial condition of the system does introduce an anisotropy. Its influence, however, on the dynamical properties of the system is still not well-understood. Thus, the BS model, being without this ambiguity about isotropicity and the sensitivity to the definition of the perimeter sites, can be regarded as the baby version of the invasion percolation model,[56] just as the directed polymer model[22] to the much more complicated spin glass model.[36]

6. Conclusion and Unsettled Problems

Finally, let us summarize the main points in the previous sections and give some possible directions for further study in the future. The data from the numerical studies of the BS evolutional model with the data from the fossil record are explicitly compared. Then, I focus on the mechanism by which the BS evolution model approaches the SOC state and the universal properties of the system at criticality, in particular, the geometric properties of avalanches, the spatial-temporal correlations between successive events and fractal pattern in the space-time plot. We see that all the exponents can be expressed in terms of D and τ, i.e. the fractal exponent of the avalanches and the avalanche size distribution exponent, respectively. The random neighbor variant offers a good pedagogical example how the mean field approach is applied and the potential danger of losing some critical properties of the original system by this approximation. Finally, I discuss the relation of the BS model to other topics, such as directed percolation, random walk, and a few self-organized critical models, and the subtle differences between them.

Some unsolved problems of this topic for further research are given in the following:

(1) As pointed out by Vandewalle and Ausloos,[55] there are some important drawbacks on the BS model definition for describing biological evolution. First, the number N of species is always kept constant. It does not allow for speciation where one species branches into two species. Secondly, an extinction is identified with the mutation. In fact, the extinction of a species may arise for reasons unrelated to a mutation event. Thirdly, the BS model does not take into account the possibility of one species competing with its own mutated species. There have been a few attempts[55,10,34,37] to modify the BS model in order to give a better description for the biological evolution. However, each of them has its own limitations. It still requires a lot of work from the statistical community to invent more realistic models.

(2) As mensioned in the context, most results in the BS model can currently only be obtained by either scaling analysis or numerical studies. Rigorous treatments on the model will be most welcomed, especially for the determination of the critical point p_c and the values of two independent critical exponents of the system, D and τ.

(3) Since it was conjectured[47,42] that the BS model is in the same universality class of directed percolation (DP), there have been a few numerical studies[23,18] casting doubt upon this conjecture. However, the discrepancy between the numerical values of the critical exponents in the BS model and those of DP is somewhat small. People might argue that this is due to the statistical deviation, finite size effects, or slow crossover behavior, etc. Therefore, a rigorous argument proving (or disproving) this conjecture is very much needed for resolving this controversy.

(4) As mentioned before, the BS model shares some similarity with self-organized interface depinning models. Especially, it can be regarded as the baby version of the invasion percolation model.[56] The extension of the BS model to higher dimensionality will not only give information regarding the model itself but also shed some lights upon these related models. The most interesting properties to be studied include the robustness of self-organized criticality, the existence of upper critical dimensionality, and the values of the critical point and the critical exponents, etc.

(5) One of the most important merits of the BS model is that it contains very rich statistical properties despite a very simple model definition. From the theoretical point of view, it will be very interesting to extend the model by varying the model definition slightly, e.g. including the next-to-nearest neighbor interaction, redefinition of the time scale, or introducing correlation to the random barriers, and then study the statistical properties of these variants, such as the robustness of self-organized criticality, the intermittent behavior, the behavior of spatial-temporal correlation, etc.

Acknowledgments

The author is very grateful to T. Halpin-Healy, F.-Y. Wu, C.-K. Hu and W.-J. Tzeng for very helpful suggestions and much encouragement. The author also gives thanks to A. Billips for her administrative assistance during the visit at Columbia University where part of this review is accomplished. This work is supported in part by the National Science Council of Republic of China under the grant number NSC 86-2112-M-002-021.

References

1. L. A. N. Amaral, A.-L. Barabási, S. V. Buldyrev, S. T. Harrington, S. Havlin, R. Sadr-Lahijany and H. E. Stanley, *Phys. Rev.* **E51**, 4655 (1995).
2. L. Anton, "*Random Walk Approach to Simple Evolution Model*", preprint (1996).

3. S. V. Buldyrev, A.-L. Barabási, F. Caserta, S. Havlin, H. E. Stanley and T. Vicsek, *Phys. Rev.* **A45**, 8313 (1992).
4. P. Bak and M. Paczuski, "*Mass Extinctions vs. Uniformitarianism in Biological Evolution*", preprint (1996).
5. A.-L. Barabási and H. E. Stanley, *Fractal Concepts in Surface Growth* (Cambridge University Press, Cambridge, 1995).
6. P. Bak, K. Chen and M. Creutz, *Nature* (London) **342**, 780 (1989).
7. J. de Boer, B. Derrida, H. Flyvbjerg, A. D. Jackson and T. Wetting, *Phys. Rev. Lett.* **73**, 906 (1994).
8. P. Bak, H. Flyvbjerg and B. Lautrup, *Phys. Rev.* **A46**, 6724 (1992).
9. J. de Boer, A. D. Jackson and T. Wetting, *Phys. Rev.* **E51**, 1059 (1995).
10. S. Boettcher and M. Paczuski, *Phys. Rev. Lett.* **76**, 348 (1996).
11. P. Bak and K. Sneppen, *Phys. Rev. Lett.* **71**, 4083 (1993).
12. P. Bak, C. Tang and K. Wiesenfeld, *Phys. Rev. Lett.* **59**, 387 (1987).
13. P. Bak, C. Tang and K. Wiesenfeld, *Phys. Rev.* **A38**, 364 (1988).
14. V. Frette, K. Christensen, A. Malthe-Sørenssen, J. Feder, T. Jøssang and P. Meakin, *Nature* **379**, 49 (1996).
15. L. Furuberg, J. Feder, A. Aharony and T. Jøssang, *Phys. Rev. Lett.* **61**, 2117 (1988).
16. H. Flyvbjerg and B. Lautrup, *Phys. Rev.* **A46**, 6714 (1992).
17. H. Flyvbjerg, K. Sneppen and P. Bak, *Phys. Rev. Lett.* **71**, 4087 (1993).
18. P. Grassberger, *Phys. Lett.* **A200**, 277 (1995).
19. S. J. Gould and N. Eldredge, *Nature* (London) **366**, 223 (1993).
20. T. E. Harris, *The Theory of Branching Processes* (Springer, Berlin, 1963).
21. S. Havlin and A. Bunde, "*Percolation*" in *Contemporary Problems in Statistical Physics*, ed. G. H. Weiss (Society for Industrial and Applied Mathematics, Philadelphia, 1994).
22. T. Halpin-Healy and Y.-C. Zhang, *Phys. Rep.* **254**, 215 (1995).
23. B. Jovanović, S. V. Buldyrev, S. Havlin and H. E. Stanley, *Phys. Rev.* **E50**, R2403 (1994).
24. T. Jonsson and J. F. Wheater, "*Avalanche Size Distribution in a Random Walk Model*", preprint (1996).
25. S. A. Kauffman, *The Origins of Order* (Oxford University Press, Oxford, New York, 1993).
26. D. E. Kellog, Paleobiology **1**, 359 (1975).
27. S. A. Kauffman and S. J. Johnsen, *Theoretical Biology* **149**, 467 (1991).
28. M. Kardar, G. Parisi and Y.-C. Zhang, *Phys. Rev. Lett.* **56**, 899 (1986).
29. S. B. Lowen and M. C. Teich, *Phys. Rev.* **E47**, 992 (1993).
30. H. Leschhorn and L.-H. Tang, *Phys. Rev.* **E49**, 1238 (1994).
31. S. Maslov, *Phys. Rev. Lett.* **74**, 562 (1995).
32. S. Maslov, "*Infinite Hierarchy of Exact Equations in the Bak–Sneppen Model*", preprint (1996).
33. S. Maslov and M. Paczuski, *Phys. Rev.* **E50**, 643 (1994).
34. S. C. Manrubia and M. Paczuski, "*A Simple Model of Large Scale Organization in Evolution*", preprint (1996).
35. S. Maslov, M. Paczuski and P. Bak, *Phys. Rev. Lett.* **73**, 2162 (1994).
36. M. Mezard, G. Parisi and M. A. Virasoro, *Spin Glass Theory and Beyond* (World Scientific, Singapore, 1987).
37. M. E. J. Newman and B. W. Roberts, *Proc. Roy. Soc. London* **B260**, 31 (1995).
38. Z. Olami, I. Procaccia and R. Zeitak, *Phys. Rev.* **E49**, 1232 (1994).
39. Z. Olami, I. Procaccia and R. Zeitak, *Phys. Rev.* **E52**, 3402 (1995).

40. N.-N. Pang, *Europhys. Lett.* **35**, 79 (1996).
41. M. Paczuski, S. Maslov and P. Bak, *Europhys. Lett.* **28**, 295 (1994).
42. M. Paczuski, S. Maslov and P. Bak, *Europhys. Lett.* **27**, 97 (1994).
43. M. Paczuski, S. Maslov and P. Bak, *Phys. Rev.* **E53**, 414 (1996).
44. D. M. Raup, *Science* **231**, 1528 (1986).
45. D. M. Raup and G. E. Boyajian, *Paleobiology* **14**, 109 (1988).
46. S. Roux and E. Guyon, *J. Phys.* **A22**, 3693 (1989).
47. T. Ray and N. Jan, *Phys. Rev. Lett.* **72**, 4045 (1994).
48. D. M. Raup and J. J. Jr. Sepkoski, *Science* **215**, 1501 (1982).
49. J. J. Jr. Sepkoski, *Paleobiology* **19**, 43 (1993).
50. K. Sneppen, P. Bak, H. Flyvbjerg and M. H. Jensen, *Proc. Natl. Acad. Sci. USA* **92**, 5209 (1995).
51. K. Sneppen, *Phys. Rev. Lett.* **69**, 3539 (1992).
52. K. Schmoltzi and H. G. Schuster, *Phys. Rev.* **E52**, 5273 (1995).
53. M. F. Shlesinger, G. M. Zaslavsky and J. Klafter, *Nature* (London) **363**, 31 (1993).
54. L.-H. Tang, *"Nonequilibrium Surfaces"* in *Annual Reviews of Computational Physics II*, ed. D. Stauffer (World Scientific, Singapore, 1995).
55. N. Vandewalle and M. Ausloos, *J. de Phys. I (France)* **5**, 1011 (1995).
56. D. Wilkinson and J. F. Willemsen, *J. Phys.* **A16**, 3365 (1983).